# RESTORING PROPULSIVE FORCES IN ELDERLY GAIT DOES NOT IMPAIR DYNAMIC STABILITY

Michael G. Browne and Jason R. Franz

University of North Carolina at Chapel Hill and North Carolina State University, Chapel Hill, NC, USA
email: mgbrowne@email.unc.edu, web: http://abl.bme.unc.edu

## INTRODUCTION

Older adults are at an exceptionally high risk of falls, and most of these falls occur during locomotor activities such as walking. Older adults may thus opt to walk slower to improve their resilience to unexpected balance challenges and mitigate their risk of falls. However, prior to eliciting slower preferred speeds, advanced age is accompanied by a precipitous reduction in propulsive forces ($F_P$) exerted during the push-off phase of walking [1]. Winter et al. (1990) originally proposed that many of the hallmark biomechanical features of elderly gait, including reductions in $F_P$ generation during push-off, reflect the adoption of a safer, more stable pattern of movement [2]. Contrary to that perspective, we recently found that a diminished push-off during walking severely compromises dynamic stability, at least in young adults [3]. Indeed, our findings alluded to unfavorable consequences of reduced $F_P$ generation on dynamic stability that could themselves precipitate slower speeds.

Together, these results suggest that mitigating age-related reductions in $F_P$ may increase dynamic stability during walking toward values seen in young adults. Indeed, although interventions often aim to restore push-off intensity (e.g., $F_P$) in older adults, it remains unclear how these changes would affect dynamic stability – a major gap in our understanding with important translational implications. Do older adults decrease propulsive force generation to attenuate their risk of falls or can we enhance push-off intensity without unfavorable effects on dynamic stability? In this exploratory study, we investigated the extent to which older adults prioritize dynamic stability in selecting their preferred push-off intensity (i.e. $F_P$ generation). We hypothesized that increasing $F_P$ generation in older adults would improve dynamic stability while decreasing $F_P$ generation would worsen dynamic stability.

## METHODS

16 older adult subjects (5 males/11 females, mean ± SD, age: 75.3 ± 3.6 years) participated this study. We first calculated subjects' preferred walking speed (PWS: 1.23 ± 0.19 m/s) using a photo cell timing system and a 10 m walkway (Bower Timing Systems, Draper, UT, USA). We then implemented a visual biofeedback paradigm based on real-time force measurements from a dual-belt force measuring treadmill (Bertec, Corp., Columbus, OH) (Fig. 1A). Specifically, for trials involving biofeedback, a custom Matlab (Mathworks, Natick, MA) script continuously computed the average bilateral peak $F_P$ during push-off from each set of four consecutive steps and projected a visual representation of those values as dots in real-time to a screen positioned in front of the treadmill (Fig. 1A).

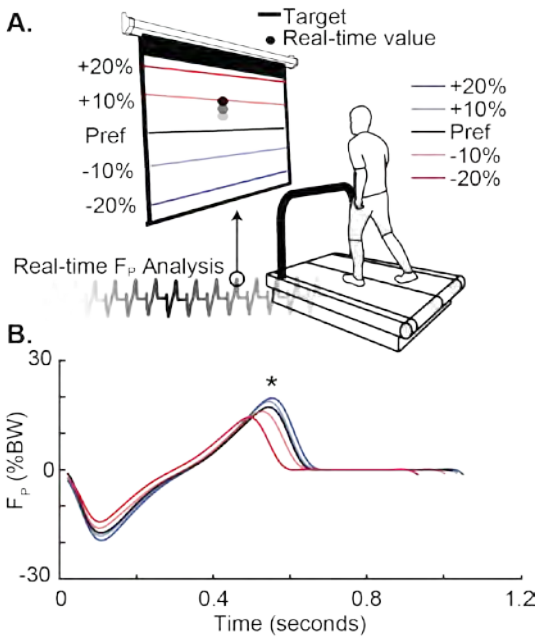


**Figure 1: A.)** Experimental design using real-time peak propulsive force measurements projected in front of participants with targets representing ±10 and 20% different from preferred. **B.)** Group average anterior-posterior ground reaction force by condition across time. Asterisks (*) denote a significant main effect of $F_P$ biofeedback ($p<0.05$).

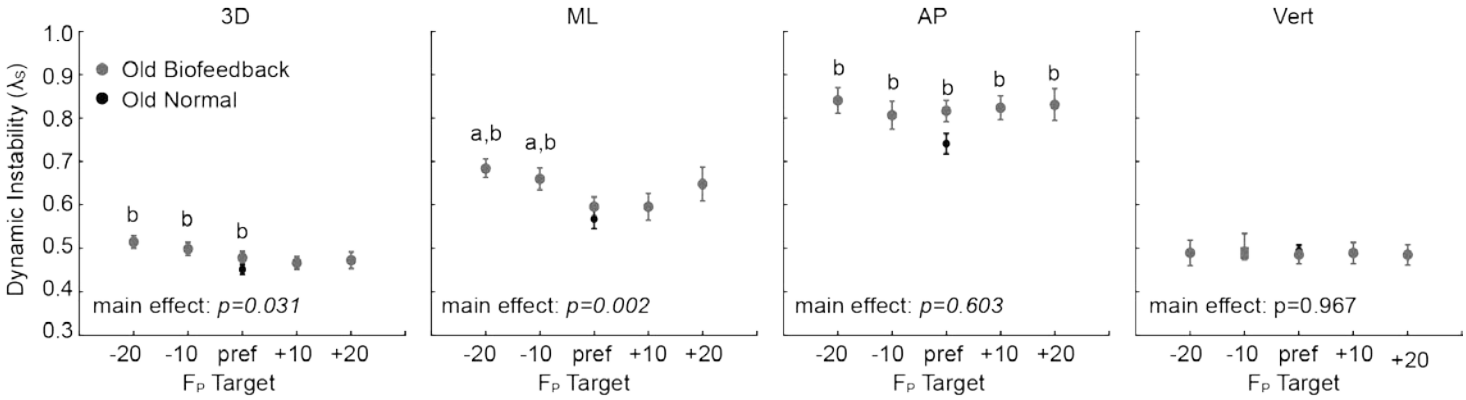


**Figure 2:** Group mean ± SE short-term maximum divergence exponents ($\lambda_S$) defined using three-dimensional (3D), mediolateral (ML), anterior-posterior (AP) and vertical (Vert) C7 velocities. 'a' and 'b' indicate significant ($p<0.05$) pairwise difference of biofeedback trial from preferred $F_P$ biofeedback and normal walking, respectively.

Subjects walked at their PWS while matching their instantaneous $F_P$ to target values representing ±10 and ±20% of preferred $F_P$ (Fig. 1B). Using motion capture data, we constructed a state vector from the time series of C7 velocity in the anterior-posterior (AP), mediolateral (ML), and vertical directions to calculate short-term maximum divergence (i.e., Lyapunov, $\lambda_s$) exponents. Finally, we analyzed the variability of C7 kinematics given its complement to dynamic stability within the context of balance control (Data not shown).

## RESULTS AND DISCUSSION

Older adults walked with a 10% $F_P$ deficit compared to previously reported values in young adults walking at similar speeds ($p<0.05$) [4]. Older adults successfully modulated their $F_P$ to target values, reaching +14% and -14% when targeting +20% and -20% different from preferred $F_P$. Older adults walked with progressively longer, wider steps across the range of presented $F_P$ targets (i.e., from -20% to +20% $F_P$). Biofeedback alone (i.e. biofeedback of preferred $F_P$) increased AP dynamic instability, and thereby, 3D instability (Fig. 2). This effect of biofeedback on divergence in the AP direction is perhaps unsurprising considering that participants have to continually modulate $F_P$ along the AP axis. Targeting decreases in $F_P$ of as little as 10% worsened (i.e., increased) ML dynamic instability compared to preferred $F_P$ biofeedback and normal walking. We posit that this is clinically meaningful; previous work suggests that older adults may be more prone to impairments in ML dynamic stability [5] and reducing $F_P$ may further exacerbate those consequences. Compared to walking with smaller than preferred $F_P$, dynamic instability was much less susceptible to walking with larger than preferred $F_P$. Interestingly, increasing $F_P$ generation in older adults, and thereby restoring push-off intensity to values seen in young adults, had no significant effect on dynamic stability. While we must reject our hypothesis that increasing $F_P$ generation in older adults would improve their dynamic stability, the absence of a negative impact when restoring older adults $F_P$ generation remains an exciting finding.

## CONCLUSIONS

Our findings suggest that restoring propulsive force generation in older adults does not negatively impact their dynamic stability. These potentially favorable results may be combined with our previous work to paint an interesting story associated with restoring push-off intensity in old age. Increasing push-off intensity in old age appears to elicit beneficial changes in joint-level biomechanics without compensatory tradeoffs in whole-body measures of balance control (i.e. dynamic stability). As such, our study builds confidence toward continued efforts to restore push-off intensity during walking in old age.

## REFERENCES

1. Franz JR, Kram R. *J Biomech* **46**, 535-40, 2013.
2. Winter D, et. Al. *Phys Ther.* **70(6)**, 340-7, 1990.
3. Browne M & Franz J. *RSOS*. 4(11): e171673, 2017.
4. Browne M & Franz *J Biomech* **55**, 48-55, 2017.
5. Cofré E, et. Al. *Gait & Posture* **42**, 79-84, 2015.

# DOES LOCAL DYNAMIC STABILITY DURING UNPERTURBED WALKING PREDICT THE RESPONSE TO BALANCE PERTURBATIONS?

Mu Qiao, Kinh N. Truong, and Jason R. Franz

University of North Carolina and North Carolina State University, Chapel Hill, NC, USA
email: jrfranz@email.unc.edu, web: http://abl.bme.unc.edu

## INTRODUCTION

Older adults are at high risk of falls, and most falls occur during locomotor activities such as walking. Reduced local dynamic stability in old age is often interpreted to suggest a lessened capacity to respond to more significant balance challenges encountered during walking and future falls risk [1]. However, it remains unclear whether local dynamic stability during normal, unperturbed walking predicts the response to larger external balance disturbances. Indeed, local dynamic stability quantifies resilience to small, naturally occurring kinematic deviations arising normally during walking, and may not reflect resilience to larger external perturbations that could elicit a fall [1]. Predicting one's resilience to external balance challenges using measurements acquired during normal, unperturbed walking may be clinically desirable, enabling the targeted prescription of preventive care. We hypothesized that larger values of local dynamic instability during unperturbed walking would positively correlate with larger changes due to optical flow perturbations – a hypothesis that we tested in subjects coalescing to provide a spectrum of walking balance integrity: young adults, older non-fallers, and older fallers.

## METHODS

We recruited 11 young (5M/6F), 11 older adult non-fallers (5M/6F), and 11 older adults with at least one fall in the last year (4M/7F) to walk on an instrumented dual-belt treadmill (Bertec, Corp.). Young adults walked at 1.25 $m \cdot s^{-1}$ while both older fallers (1.03±0.22 $m \cdot s^{-1}$) and non-fallers (1.19±0.20 $m \cdot s^{-1}$) walked at their preferred overground speed. While walking, subjects watched a speed-matched, virtual hallway rear-projected onto an immersive semi-circular curved screen surrounding the treadmill (Fig. 1A) both with and without continuous oscillations of optical flow designed to elicit the visual perception of lateral instability [2]. In randomized order, subjects walked for 2 min normally and with optical flow perturbations at amplitudes of 20, 35, and 50 cm. A 14-camera motion capture system (Motion Analysis Corp., 100Hz) recorded the 3D trajectories of heel markers and the C7 vertebrae (filtered with a low-pass cutoff of 8 Hz). We quantified local dynamic stability by estimating maximum exponential rates of divergence (*i.e.*, λ, bits·stride$^{-1}$) from 3D C7 marker velocity time series (Eqn. 1). We constructed a state space, $\boldsymbol{S}(t)$, as:

$$\boldsymbol{q}(t) = (\dot{x}, \dot{y}, \dot{z}) \quad (1)$$

$$\boldsymbol{S}(t) = [\boldsymbol{q}(t), \boldsymbol{q}(t + 1 \cdot \tau), \cdots, \boldsymbol{q}(t + (d_E - 1)\tau)] \quad (2)$$

where, $\dot{x}, \dot{y},$ and $\dot{z}$ are the C7 velocity components in the anterior-poster, medio-lateral, and vertical directions, respectively. By convention [1,2], we computed the maximum rates of divergence of initially neighboring trajectories from $\mathbf{S}(t)$ using an embedding dimension ($d_E$) of 4 and a time delay (τ) equal to one quarter of subjects' average stride time. We time normalized the divergence curves to account for differences in stride period and calculated short-term (i.e., $\lambda_S$, 0 to 1 stride) and long-term (i.e., $\lambda_L$, 4 to 10 stride) divergence exponents for each condition, where larger positive values indicate larger local dynamic instability. A mixed 2-way factorial ANOVA first tested for main effects of group and condition on $\lambda_S$ and $\lambda_L$ using α=0.05. Linear regressions then estimated the relation

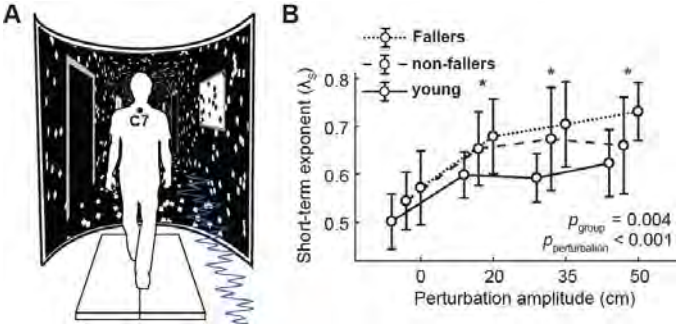


**Figure 1**: (A) Virtual environment. (B) The effects of group (*e.g.,* young adults, non-fallers, and fallers) and perturbation amplitude on short-term local divergence exponents ($\lambda_S$).

between local dynamic stability during unperturbed walking ($\lambda_{unperturbed}$) and the average change thereof in response to perturbations (i.e., $\bar{\lambda}_{perturbed}$-$\lambda_{unperturbed}$).

## RESULTS AND DISCUSSION

*Aging and falls history effects on dynamic instability*

We observed a significant effect of group on short-term ($\lambda_S$, $p$=0.004, Fig. 1B) but not long-term local dynamic instability - an effect governed by instability due to age, independent of falls history. However, neither age nor falls history significantly affected dynamic instability during unperturbed walking. Compared to unperturbed walking, optical flow perturbations significantly increased short-term ($\lambda_S$, $p$<0.0001, Fig. 1B) local dynamic instability – which affected all subject groups (young: $p$<0.001, non-fallers: $p$=0.009, fallers: $p$<0.001, Fig. 1B).

Perturbations revealed between-group differences in local dynamic instability that were not apparent during unperturbed walking. Age alone did not increase local dynamic instability during walking for any optical flow perturbation amplitudes. In contrast, fallers exhibited larger local dynamic instability than young adults for all three perturbation amplitudes (fallers *vs*. young: $p$<0.009, Fig. 1B). We observed no difference in local dynamic instability between fallers and non-fallers for the two smallest amplitude perturbations ($p$≥0.445, Fig. 1B). However, although not statistically significant, fallers tended to have larger local dynamic instability than non-fallers at the largest amplitude (50cm: $p$=0.059, Fig. 1B).

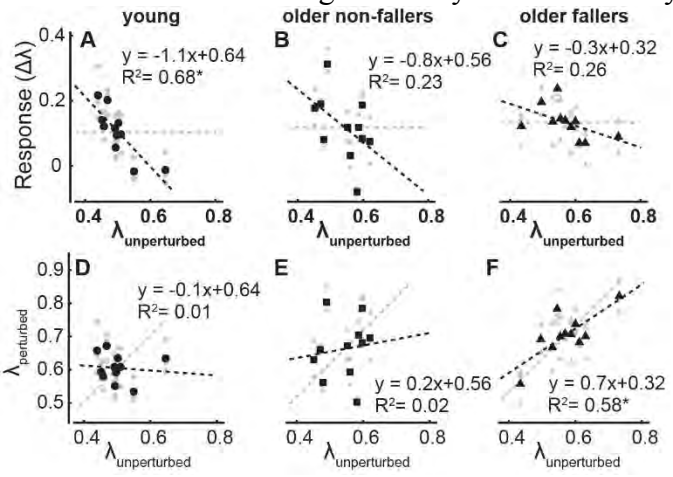


**Figure 2.** Top row; correlations between $\lambda_S$ during unperturbed walking ($\lambda_{unperturbed}$) and the average change thereof in response to perturbations ($\Delta\lambda$=$\lambda_{perturbed}$-$\lambda_{unperturbed}$) for (A) young adults, (B) older non-fallers, and (C) older fallers. Bottom row; correlations between $\lambda_{unperturbed}$ and the average in response to optical flow perturbations ($\lambda_{perturbed}$) for (D) young adults, (E) older non-fallers, (F) and older fallers. The black dashed line is the best linear fit; the solid gray line has a slope of zero (top row) or one (bottom row) indicating, in both, a response to perturbations that is independent of subjects' baseline stability.

*Predicting the response to balance perturbations*

The relation between $\lambda_S$ during unperturbed walking and changes due to optical flow perturbations differed across individual groups (Fig. 2). Young adults had the only significant. and by far the strongest and steepest, negative correlation between local instability during unperturbed walking and response to perturbations ($R^2$=0.68, Fig. 2A). Compared to young adults, this relation was similarly steep but much less well correlated in older non-fallers ($R^2$=0.23, Fig. 2B). Finally, older fallers exhibited by far the most shallow regression between $\lambda_S$ during unperturbed walking and changes thereof due to optical flow perturbations ($R^2$=0.26, Fig. 2C). Indeed, the relation between $\lambda_S$ during perturbed and unperturbed walking reached significance and approximated the line of unit only for older fallers, indicating a uniform response that emerged only in older adults with a history of falls (Fig. 2F).

## CONCLUSIONS

Although modest, our data first suggest that older adults with a history of at least one fall have a more pervasive susceptibility to optical flow perturbations than older non-fallers during walking. Second, in surprising contrast to our hypothesis, a significant negative correlation indicated that young adults with higher local dynamic instability during unperturbed walking exhibited *smaller* responses to optical flow perturbations. One interpretation is that young adults may self-regulate their response to balance perturbations based on a self-perception of risk guided by their baseline level of dynamic instability. In contrast, particularly among older fallers, the response to optical flow perturbations appeared completely independent of their baseline level of dynamic instability. We conclude that understanding the response to balance perturbations, especially among older fallers, may require measuring that response directly rather than relying on measures collected during normal, unperturbed walking


## ACKNOWLEDGEMENTS

Supported by a grant from NIH (R56AG054797)


## REFERENCES


[1] Kang and Dingwell, J Biomech 14; 2008.

[2] Franz et al., Hum Mov Sci 40; 2015.

# GAIT ASYMMETRIES 6 MONTHS POST-ACLR ASSOCIATE WITH INTER-LIMB T1ρ RATIOS 12 MONTHS POST ACLR

[1]Steven J. Pfeiffer, [1]Jeffrey Spang, [1]Daniel Nissman, [1,2]David Lalush, [1]Kyle Wallace, [3]Matthew S. Harkey, [1]Laura Stanley, [4]Randy Schmitz, [1]Troy Blackburn, [1]Brian Pietrosimone

[1] University of North Carolina at Chapel Hill, Chapel Hill, NC, USA, [2] North Carolina State University, Raleigh, NC, USA, [3]Tufts Medical Center, Boston, MA, USA, [4]University of North Carolina at Greensboro, NC, USA. email: stevenpf@email.unc.edu

## INTRODUCTION

Individuals who sustain an anterior cruciate ligament injury and reconstruction (ACLR) are at heightened risk for posttraumatic knee osteoarthritis (PTOA).[1] The progression to PTOA following ACLR is theorized to result from an interaction between aberrant joint biomechanics during walking and deleterious biological changes to the knee cartilage.[2] Alterations in proteoglycan density within the cartilage matrix are hypothesized to be one of the initial cartilage changes that may be related to PTOA development.[3] T1ρ magnetic resonance imaging (MRI) relaxation times are sensitive to proteoglycan density changes and are elevated, indicating worse proteoglycan density, as early as one year post-ACLR.[4] The purpose of this study was to determine the associations between limb symmetry indices (LSI) for gait biomechanics measured six months post-ACLR and femoral T1ρ relaxation times twelve months post-ACLR. We hypothesized individuals with lesser loading of the ACLR limb six months following ACLR would demonstrate greater T1ρ MRI relaxation times on the ACLR limb twelve months following surgery.

## METHODS

Twenty-four individuals (50% female, 21.92 ± 3.61 years old, 178.13 ± 11.30 cm, 75.35 ± 12.60 kg) with a unilateral bone-patellar-bone autograft ACLR participated in this study. Walking biomechanics [peak vertical ground reaction force (vGRF), vGRF loading rate (vGRF-LR), and peak internal knee extension moment (KEM)] were extracted from the first 50% of stance phase in both limbs during five trials of walking at self-selected speed six months following ACLR. LSI were used to normalize the biomechanical outcomes of the ACLR limb to the uninjured limb (ACLR Limb / Uninjured limb). Peak vGRF (BW) and vGRF-LR (BW/s) were normalized to body weight. vGRF-LR was calculated as the peak of the first derivative of the force-time curve. KEM was calculated using an inverse dynamics approach and was normalized to the product of body weight and height (BW*m). KEM was expressed as an internal moment and a negative value.

A 3-Tesla scanner was used to acquire images following 30 minutes of unloading the knee joint. T1ρ relaxation times were calculated (Figure 1) for the medial and lateral femoral condyles (MFC & LFC) using a five-image sequence created with a MatLab program with the following equation: $S(TSL) = S0 \exp(-TSL/T1\rho)$ where TSL is the duration of the spin-lock time, S0 is signal intensity when TSL equals zero, S corresponds to signal intensity, and T1ρ is the T1 relaxation time in the rotating frame. Prior to segmentation, affine and non-rigid deformable registration techniques were utilized to align the ACLR limb to the uninjured limb. The weight bearing portions of the cartilage of the MFC and LFC was manually segmented into posterior, central, and anterior regions of interest (ROI) based on the location of the meniscus in the sagittal plane.[5] Inter-limb T1ρ relaxation time ratios (T1ρ ILR = ACLR limb T1ρ / uninjured limb T1ρ) were calculated for each ROI.

**Figure 1:** Representative map of T1ρ relaxation times of an ACLR (L) and contralateral (R) knee.

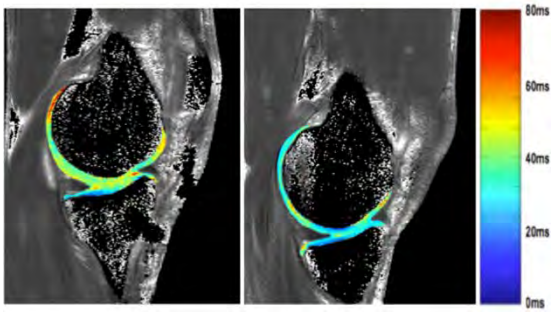

Separate, stepwise linear regressions were used to determine the unique associations between knee biomechanical outcomes and ILR for each ROI ($\Delta R^2$, $\beta$, $P \leq 0.05$). Self-selected gait speed and the presence of a meniscal injury may influence T1ρ MRI relaxation times following ACLR. Therefore, these variables were entered into the regression model first followed by the biomechanical variable of interest. The presence of a medial or lateral meniscal injury was entered when specifically evaluating ILR of cartilage in either the medial or lateral compartment, respectively.

## RESULTS

Lesser peak vGRF LSI six months following ACLR significantly associated with greater Posterior-LFC T1ρ ILR ($\Delta R^2$=0.20, $\beta$=-0.48, P=0.04) twelve months following ACLR. Similarly, lesser peak vGRF-LR LSI six months following ACLR significantly associated with greater Posterior-MFC T1ρ ILR ($\Delta R^2$=0.19, $\beta$=-0.45, P=0.05) twelve months following ACLR. Additionally, lesser peak KEM LSI six months following ACLR significantly associated with greater Central-MFC T1ρ ILR ($\Delta R^2$=0.19, $\beta$=0.46, P=0.04) twelve months following ACLR.

## DISCUSSION

Consistent with our hypothesis, individuals with lesser peak vGRF LSI, vGRF-LR LSI, and peak internal KEM LSI during walking six months following ACLR, demonstrated greater T1ρ ILR in the medial and lateral femoral condyles. These findings suggest that lesser mechanical loading of the ACLR limb compared to the uninjured limb early (i.e. 6 months) following ACLR may be related to deleterious changes in proteoglycan density of the ACLR limb compared to the uninjured limb at a later time point following ACLR (i.e. 12 months).

Both excessive and insufficient mechanical loading of the knee can lead to breakdown of tibiofemoral cartilage within the joint. Recent evidence[6,7] has demonstrated that excessive mechanical loading during walking early following ACLR associates with increased T1ρ relaxation times at early and later time points following ACLR. The findings of the current study are contrary to these studies but are consistent with previous findings demonstrating that lesser mechanical loading during walking following ACLR associates with changes in cartilage metabolism,[8] structure,[9] and future PTOA development.[10] Future work is needed to further understand the association between joint loading and deleterious changes to joint tissue metabolism following knee joint injury in order to develop interventions to optimally load the joint for the purpose of improving long-term joint health.

## CONCLUSIONS

The findings of the current study illustrate that mechanical loading, specifically lesser loading, between limbs during walking early following ACLR may be related to deleterious changes of the cartilage matrix at later time points following ACLR, which may be related to the development of future PTOA. These findings illustrate the need for establishing optimal mechanical loading patterns during walking early in the rehabilitation process.

## REFERENCES


1. Luc B, et al. *Journal of Athletic Training*. 2014;49(6):806-819.
2. Andriacchi TP, et al. *Annals of Biomedical Engineering*. 2015;43(2):376-387.
3. Regatte RR, et. al. *Academic Radiology*. 2002;9(12):1388-1394.
4. Regatte RR, et al. *Journal of Magnetic Resonance Imaging*. 2006;23(4):547-553.
5. Pfeiffer S, et al. *Arthritis Care and Research (Hoboken)*. 2017.
6. Kumar D, et al. *American Journal of Sports Medicine*. 2018;46(2):378-387.
7. Teng HL, et al. *American Journal of Sports Medicine*. 2017: 45(14): 3262–3271.
8. Pietrosimone B, et al. *Journal of Orthopedic Research*. 2017. 35(10): 2288–2297
9. Saxby DJ, et al. *Orthopedic Journal of Sports Medicine*. 2017;5(8).
10. Wellsandt E, et al. American Journal of Sports Medicine. 2016;44(1):143-151.

# OLDER ADULTS REVERSE THEIR DISTAL-TO-PROXIMAL REDISTRIBUTION USING BIOFEEDBACK

Michael G. Browne, Sarah N. Fickey, and Jason R. Franz

University of North Carolina at Chapel Hill and North Carolina State University, Raleigh, NC, USA
email: mgbrowne@email.unc.edu, web: http://abl.bme.unc.edu

## INTRODUCTION

Compared to young adults, older adults walk slower and with a characteristic decrease in push-off intensity. This decreased push-off intensity stems from large reductions in mechanical power generated by the plantarflexor muscles (i.e. ankle power, $P_A$) and propulsive ground reaction forces generated during push-off ($F_P$) [1]. Seemingly in response to this decreased push-off intensity, older adults also rely more on positive mechanical power generated by the hip musculature. This phenomenon, known as the distal-to-proximal redistribution [2], may also contribute to increased metabolic energy costs during walking in older adults [3]. Conventional resistance training for improved mobility in older adults successfully improves maximal muscle strength and fast walking speed (FWS) but has minimal functional impact on habitual walking performance (i.e. preferred walking speed; PWS) or gait biomechanics (e.g., mechanical power generation).

Rehabilitative approaches that go beyond resistance training alone are needed, toward more direct means to elicit favorable biomechanical adaptations during habitual speed walking. As an important first step, we previously attempted to enhance push-off intensity in older adults using biofeedback to increase propulsive forces. While effective - older adults increased $F_P$ with potentially favorable reductions in hip flexor power generation [4] – we were surprised to observe no concomitant increase in $P_A$. However, older adults can increase $P_A$ in order to walk faster or uphill, revealing a translationally important gap in our understanding. Motivated by these findings, we tested here the primarily hypothesis that real-time ankle power biofeedback during walking can directly increase $P_A$ in older adults. We also hypothesized that doing so would: (*i*) alleviate mechanical power demands at the hip and (*ii*) increase preferred but not fast walking speed.

## METHODS

10 healthy older adults (mean±SD; age: 74.8±5.4 years, 3 males/7 females) participated in this study. We first assessed subjects' PWS (1.28±0.20 m/s) and FWS (1.79±0.20 m/s) using an instrumented walkway. Subjects then walked normally for 1-min on a dual-belt instrumented treadmill at their PWS. A custom Matlab script running a surrogate inverse dynamic model of the lower legs and feet estimated bilateral step-by-step $P_A$. Subjects walked again for 1-min each while watching a screen with visual biofeedback of their instantaneous $P_A$ and targeting increases of +10% and +20% of normal (Fig. 1A). For all trials, a motion capture system recorded the

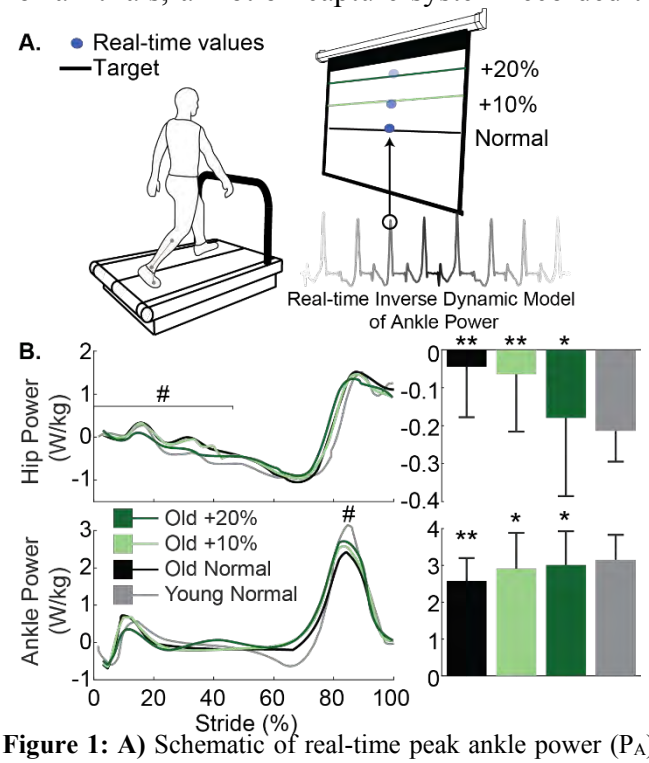


**Figure 1: A)** Schematic of real-time peak ankle power ($P_A$) biofeedback. **B)** Group-mean hip and ankle power plotted against an averaged gait cycle. Pound signs (#) denote a significant main effect of $P_A$ biofeedback ($p<0.05$). Each graph is accompanied by bar graphs indicating group mean (±SD) peaks. Asterisks (*) and double asterisks (**) denote a significant pairwise difference from old and young adults walking normally, respectively.

trajectories of markers placed on subjects' pelvis and lower extremities for estimating joint kinetics. Data reported represents the 20 consecutive strides for which participants were most successful matching prescribed targets. Finally, we again assessed subjects' PWS and FWS to investigate recall. We additionally include normal walking data from 9 healthy young adults (age: 25.1±5.6 years, 4 males/5 females, PWS: 1.30±0.12 m/s) to serve as a reference for comparison.

## RESULTS AND DISCUSSION

Our older adults walked with 21% lower $P_A$ and 79% greater hip power during early to mid-stance compared to their younger counterparts ($p<0.034$). Older adults increased $P_A$ by 13% and 17% when targeting increases of 10% and 20%, respectively (main effect, $p=0.006$), thereby attenuating their $P_A$ deficit compared to young adults (Fig. 1B). Conceptually, older adults could increase $P_A$ through changes in net moment or angular velocity at the ankle. Our older adult subjects increased $P_A$ through modest (+3%) but significant changes to peak ankle moment ($p=0.008$) and nonsignificant changes to angular velocity (+7%, $p=0.157$) (Fig. 2). We also observed larger net ankle moments developed during early to midstance, which may have indirectly contributed to larger than preferred $P_A$ through greater elastic energy storage and return. Greater $P_A$ was also accompanied by up to a 300% reduction in the demand for positive hip power generation during early to mid-stance ($p=0.015$). $P_A$ biofeedback also increased positive ankle joint work ($p=0.001$), total positive leg joint work ($p=0.002$), and $F_P$ ($p<0.001$) (Fig. 2). This latter finding reveals an interesting disconnect in our understanding of push-off in walking: older adults increase $F_P$ without related improvements in $P_A$ [4], but increase $P_A$ with related improvements in $F_P$. Finally, subjects walked overground with 11% faster PWS ($p=0.010$) but no change in FWS when recalling $P_A$ biofeedback.

## CONCLUSIONS

Our results reveal that older adults are capable of increasing $P_A$ through the use of targeted ankle power biofeedback – effects that are accompanied by potentially favorable shifts in hip power generation during early to mid-stance. Moreover, the associated

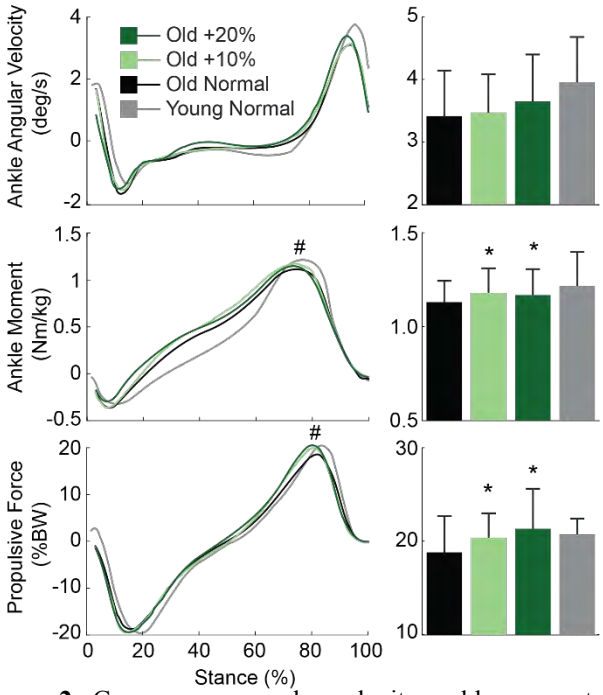


**Figure 2:** Group mean angular velocity, ankle moment, and propulsive force ($F_P$) against an average gait cycle. Asterisks (*) denote a significant main effect of biofeedback ($p<0.05$). Each graph is accompanied by bar graphs indicating group mean (±SD) peaks. Asterisks (*) denote a significant pairwise difference from old adults walking normally.

increase in PWS suggests a functional benefit to increased ankle power output during habitual speed walking. Further work will investigate whether ankle angular velocity alone may be sufficient feedback to modulate $P_A$, an approach more immediately translatable to novel rehabilitation approaches via wearable sensor technologies. Ultimately, targeted biofeedback may complement resistance training to reverse age-associated mobility decline.

## REFERENCES


1. Franz, JR. *Exercise and sport science reviews,* 44(4):129-35, 2016.
2. DeVita, P & Hortobagyi, T. *J Appl Physiol*, 88(5):1804-11, 2000.
3. Ortega, JD & Farley, CT. *J Appl Physiol*. 102(6):2266-73, 2007.
4. Browne, MG & Franz, JR. *Plos One*. In Review, 2018.


## ACKNOWLEDGEMENTS


This work was supported by grants from NIH (R01AG051748) and the UNC University Research Council.

# TRICEPS SURAE MUSCLE-SUBTENDON INTERACTION DIFFERS BETWEEN YOUNG AND OLDER ADULTS

William H. Clark and Jason R. Franz

University of North Carolina and North Carolina State University, Chapel Hill, NC, USA
email: jrfranz@email.unc.edu, web: http://abl.bme.unc.edu

## INTRODUCTION

Mechanical power generated via triceps surae muscle-tendon interaction during walking is largely responsible for the total power needed for forward propulsion and swing initiation [1]. This interaction is made complex by the biological architecture of the Achilles tendon (AT), which consists of distinct bundles of tendon fascicles, known as "subtendons", arising from the gastrocnemius (GAS) and soleus (SOL) muscles [2]. Comparative data and our own *in vivo* evidence alludes to a reduced capacity for sliding between adjacent subtendons compromising the AT in old age. This is functionally important, as subtendon sliding could facilitate independent actuation between individual triceps surae muscles, perhaps augmenting contributions to trunk support and forward propulsion. Indeed, our lab recently found that an age-associated reduction in the capacity for sliding between GAS and SOL subtendons correlated with smaller peak ankle moments and positive work performed during push-off, alluding to unfavorable functional consequences [3]. However, it remains unclear whether age-associated changes at the subtendon level unfavorably affect triceps surae muscle contractile dynamics. Recently, we introduced a novel dual-probe ultrasound imaging approach to reveal that length change differences between the GAS and SOL of young adults during force generation positively correlated with non-uniform tissue displacement patterns in the AT.

Therefore, the purpose of this study was to investigate aging effects on triceps surae muscle-subtendon interaction dynamics using dual-probe ultrasound imaging during a series of ramped isometric contractions. We hypothesized that, compared to young adults, older adults will have (*i*) more uniform Achilles subtendon tissue displacements that (*ii*) are accompanied by more uniform GAS and SOL muscle length change dynamics.

## METHODS

We report data for 9 younger adults (age: 25.1 ± 5.6 years, weight: 69.8 ± 6.9 kg, height: 1.7 ± 0.1 m, 4 females) and, thus far, 6 older adults (age: 74.3 ± 3.4 years, weight: 67.2 ± 9.0 kg, height: 1.7 ± 0.1 m, 4 females). Subjects completed 3 ramped isometric voluntary contractions at each of 5 different ankle angles (spanning 30° plantarflexion to 10° dorsiflexion) using a Biodex (Biodex System 4 Pro), with the knee flexed to replicate that near the push-off phase of walking (~20º). We synchronized two linear array ultrasound transducers to simultaneously record GAS and SOL fascicle kinematics with tissue displacements in their associated tendinous structures (Fig. 1). A 60 mm Telemed Echo Blaster 128 transducer (LV7.5/60/128Z-2) placed over the medial gastrocnemius and soleus of subjects' right leg recorded cine B-mode images at 61 frames/s. Simultaneously, a 38-mm transducer (L14-5W/38, Ultrasonix Corporation, Richmond, BC) operating at 70 frames/s recorded ultrasound radiofrequency (RF) data from a longitudinal cross-section of the right free AT, distal to the SOL muscle-tendon junction and secured via a custom orthotic. Subjects' right foot was barefoot throughout the experiment to facilitate proper placement of the AT transducer.

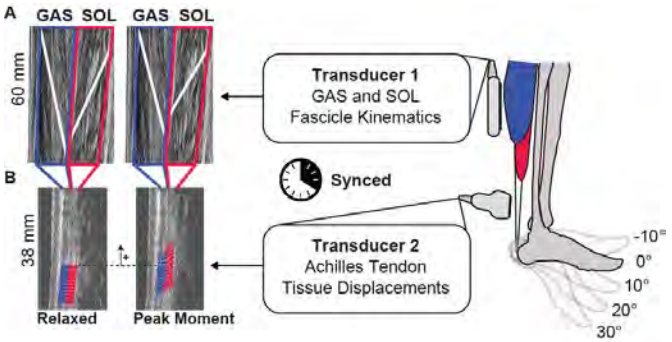


**Figure 1.** Simultaneous ultrasound imaging of the gastrocnemius (GAS), soleus (SOL), and Achilles free tendon. (A) Fascicle lengths and pennation angles derived from cine B-mode images. (B) Custom speckle-tracking of localized Achilles tendon tissue displacements.

Finally, motion capture tracked right ankle and knee joint kinematics and the positions and orientations of both probes.

Available MATLAB routines based on an affine extension to an optic flow algorithm quantified time series of GAS and SOL fascicle lengths and pennation angles (UltraTrack, [4]), which we combined to compute longitudinal muscle lengths. A custom 2D speckle-tracking algorithm estimated localized displacements of AT tendon tissue, which we averaged in two equally sized tendon depths - superficial and deep - corresponding to tendon tissue thought to arise from GAS and SOL, respectively [5]. A repeated measures ANOVA tested for, in part, significant main effects of and interactions between age and ankle angle on GAS-SOL differences in muscle shortening and tendon tissue displacement at peak ankle moment using an alpha level of 0.05.

## RESULTS AND DISCUSSION

For young and older adults, peak isometric plantarflexor moment decreased progressively from dorsiflexion to plantarflexion across the angles tested ($p$<0.01). On average, older adults generated a 21% smaller peak isometric plantarflexor moment than young adults ($p$=0.014). Compared to young adults, average peak muscle shortening was 21% greater for SOL and 81% greater for GAS, while average peak tendon displacement was 18% greater for SOL and 50% greater for GAS in older adults (Fig. 2) – findings fully consistent with functional consequences of increased compliance in older tendon. In addition, consistent with our translational premise, GAS versus SOL differences in muscle contractile behavior and those in subtendon tissue displacements were significant in young but not in older adults. Indeed, as hypothesized, differences between peak GAS subtendon and peak SOL subtendon displacement averaged 44% smaller in older versus young adults (e.g., 77% at 0º, $p$<0.05). Also as hypothesized, differences between peak SOL and peak GAS muscle shortening averaged 58% smaller in older versus young adults (e.g., 65% at 0º, $p$<0.05) (Fig. 2).

## CONCLUSIONS

We reveal that more uniform AT tissue displacements in older versus young adults extend to anatomically consistent and potentially unfavorable changes in muscle contractile behavior – evidenced by smaller differences between GAS and SOL peak shortening during isometric force generation. These findings provide an important biomechanical basis for previously reported correlations between more uniform AT subtendon behavior and reduced ankle moment generation during waking in older adults.

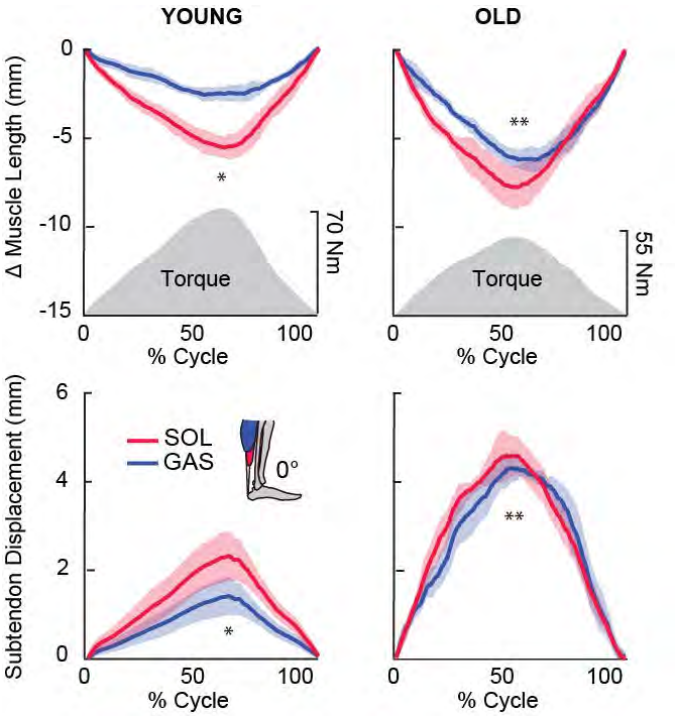


**Figure 2.** Group mean muscle shortening (above) and subtendon displacements (below; proximal positive). Gray shaded regions show the group mean net torque profile during a loading-unloading cycle. Single asterisks (*) indicate significant difference between peak GAS and peak SOL, Double asterisks (**) indicate significant difference between young and old. $p$<0.05 significant.

## REFERENCES


[1] Zelik, K.E., et al. *J Theor Biol*, 2014.75-85.
[2] Szaro, P., et al. *Ann Anat*, 2009. (**6**):586-93.
[3] Franz, J.R., et al. *J Appl Physiol* (1985), 2015. (3):242-9.
[4] Farris, D.J., et al. *Comput Methods Programs Biomed*, 2016.111-8.
[5] Franz, J.R., et al. *Gait Posture*, 2015. (**1**):192-7.


## ACKNOWLEDGEMENTS


We thank Ashish Khanchandani, Hannah Mckenney, and Michael Browne for their assistance with data collection. This study was supported by a grant from NIH (R01AG051748).

# POST-STROKE WALKING MECHANICS USING A SPEED-ADAPTIVE MYOELECTRIC EXOSKELETON CONTROLLER

[1] Emily M. McCain, [1]Tracy N. Giest, [1]Katherine R. Saul, [2]Taylor J.M. Dick and [3]Gregory S. Sawicki

[1] North Carolina State University, Raleigh, NC, USA
[2] University of Queensland, St Lucia, QLD, Australia
[3] Georgia Institute of Technology, Atlanta, Georgia, USA
email: emmccain@ncsu.edu

## INTRODUCTION

Reduced ankle function in post-stroke individuals limits the propulsive 'push-off' power of the paretic limb, resulting in asymmetric gait, reduced walking speed and higher metabolic cost [1]. Powered exoskeletons (exos) offer a promising opportunity to restore mechanical deficits by applying torque at the paretic ankle during the propulsive phase of gait. Previously, a proportional myoelectric ankle exo was shown to increase the paretic plantarflexion moment for stroke survivors walking at 75% of their comfortable overground speed [2]. Despite these improvements, the exos did not reduce the metabolic cost of walking. Researchers suggested exo performance could be limited because the walking speed was restricted to a pace at which exo assistance was not needed. In order to assess the impact of exo assistance on walking speed in stroke populations, we developed a novel, speed-adaptive exo controller [3]. This research extends previous work by: (i) exploring the efficacy of a myoelectric exo controller that automatically modulates the magnitude of propulsive assistance with changes in walking speed for post-stroke populations and (ii) assessing the ability of the controller to improve net average mechanical power output at the paretic ankle, knee and hip joints.

## METHODS

We implemented a speed-adaptive controller designed to mitigate specific limitations of prior myoelectric controllers by including two independent adaptive gains: (1) a gain to map user's soleus muscle activity to peak exo torque (Koller) and (2) a gain to map peak exo torque capacity to walking speed (Giest) [3,4]. The speed-dependent gain ensures the exo outputs ~25% of the maximum normal biological ankle plantarflexion moment at the instantaneous treadmill velocity. The desired exo torque profile was applied by a benchtop motor (Baldor Electric Co) to the carbon-fiber ankle exo through a Bowden-cable transmission system.

Experimental data were collected from six stroke survivors (3 male, 3 female) walking on an instrumented split belt treadmill with and without an exo on their paretic limb. Subjects started by walking at 60% of their preferred speed (n00). At each consecutive minute, the treadmill speed was increased by 0.1 m/s (n01, n02, etc) until the subject's heart rate reached 60% of their heart rate reserve. Kinematic and kinetic data were processed in Visual3D (CMotion, USA) and MATLAB (Mathworks, USA) to determine joint angles and angular velocities. Inverse dynamics was used to calculate joint moments and powers at the ankle, knee, and hip. Average joint powers were calculated at the ankle, knee and hip for five strides [5]. Indirect calorimetry was used to determine metabolic cost during walking (OxyCon Mobile, Carefusion, USA). Statistical significance of peak average ankle power, and net average ankle, knee and hip powers were determined using paired t-tests ($\alpha$=0.05).

## RESULTS AND DISCUSSION

The speed-adaptive controller successfully amplified exo assistance as walking speed was increased, verifying efficacy of the speed-adaptive gain (Figure 1c). Subject averages for maximum paretic ankle power were significantly higher for the exo compared to the no exo condition at all speeds (Figure 1a and 1b) (paired t-test; p=0.04). Since subjects walked until reaching a specific heartrate, statistical power was reduced at high speeds for which the sample size was small (n<4 for n05-n07).

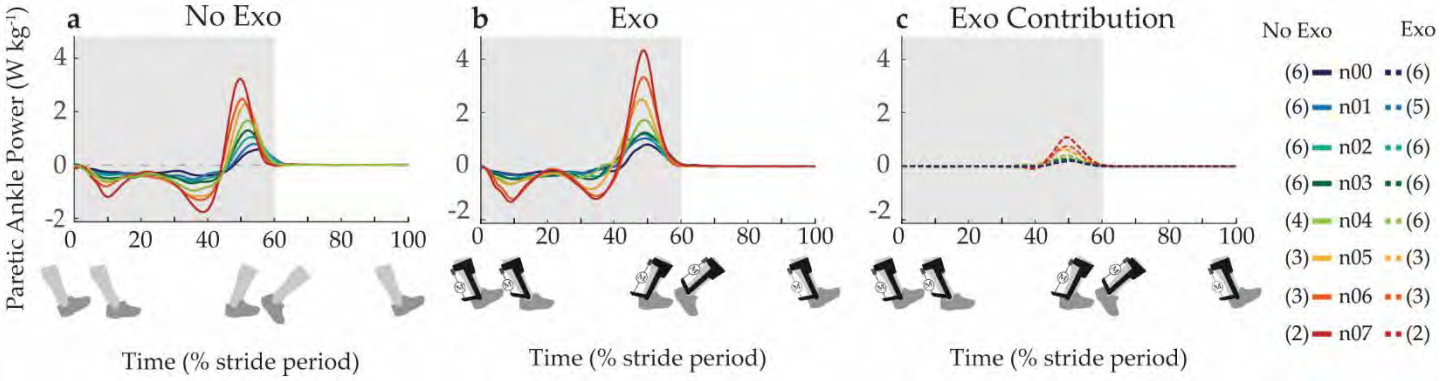


**Figure 1.a** Paretic ankle power in the no exo condition and **1.b** the exo condition with the **1.c** exo contribution isolated. The number of subjects is indicated in parenthesis. The shaded area represents the stance phase of gait.

Net average paretic ankle power was increased for all speeds while wearing the exo, demonstrating improved delivery of net energy at the ankle (paired t-tests; $p<0.05$ for n00-n04) (Figure 2).

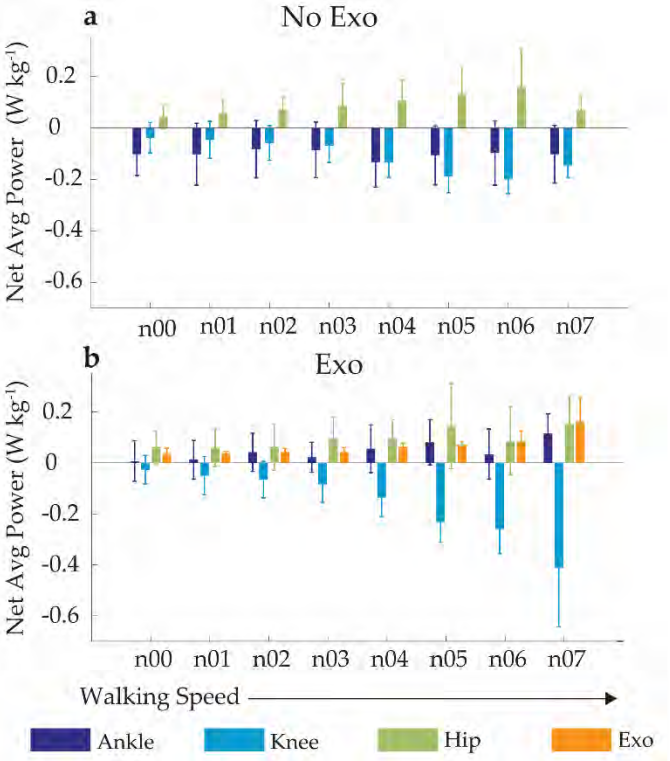


**Figure 2.a** Net average power averaged across subjects for the no exo and **2.b** exo conditions.

Despite these increases in net average ankle power, only two of the subjects experienced a decrease in metabolic cost while wearing the exo compared to the no exo condition, and no statistically significant change was found. One possible explanation is that assistance applied at the ankle may be absorbed by more proximal joints. This explanation is supported by the decrease in net average power seen at the knee in the exo compared to no exo condition (paired t-tests; $p<0.05$ for n00 and n02) (Figure 2).

## CONCLUSIONS

Our speed-adaptive controller successfully increased exo assistance with changes in walking speed for post-stroke individuals. The exo assistance resulted in higher net average power at the paretic ankle. Though we found no significant change in metabolic cost, our exo controller demonstrates the potential of assistive devices to restore paretic limb propulsive power. Future work will examine the interaction between exo assistance, walking speed, distance travelled and gait symmetry between paretic and non-paretic limbs.

## REFERENCES

1. Peterson, CL et al. *J Biomech*. 2010; 43:2348–55.
2. Takahashi, KZ et al. *J NeuroEng Rehab*.2015;12:23
3. Giest, TG et al. *ASB Abstract*, 2016.
4. Koller, JR et al. *J NeuroEng Rehab* 2015; 12:97.
5. Farris, DG et al. *J NeuroEng Rehab* 2015; 12:24.

## ACKNOWLEDGEMENTS

We would like to acknowledge Dr. RW Nuckols for his assistance developing and implementing the controller. Funded by the National Institutes of Health, National Institute for Child Health and Human Development. NIH grant R21 HD072588-01A1 to GSS.

# GLENOHUMERAL JOINT STABILITY DURING DYNAMIC PUSHING AND PULLING

Daniel C. McFarland, Emily M. McCain, Michael N. Poppo, and Katherine R. Saul

North Carolina State University, Raleigh, NC, USA
email: dcmcfarl@ncsu.edu

## INTRODUCTION

The glenohumeral joint is the most mobile joint in the human body and depends on active contributions of muscles to stabilize the resultant joint reaction force (JRF) within the glenoid fossa [1]. JRFs composed of large ratios of transverse to compressive forces destabilize the joint and pose a greater risk for shoulder dislocations. Prior dislocations can damage the fibrous structures surrounding the glenoid fossa [1] and reduce the stability index during hand-positioning tasks [2]. Therefore, to prevent degenerative wear to the joint, workspace design should consider glenohumeral instability to avoid motions that naturally place the shoulder at higher risk for instability. Pushing is a common industrial task that has been shown to have increased transverse to compressive forces [2,3]. Knowledge of whether these risks are spatial dependent with task target could be used to design safer workspaces. Our goal was to evaluate how task direction and task target during dynamic push-pull tasks influence joint reaction loads.

## METHODS

Prior experimental data of 18 subjects (9M/9F) performing a series of push and pull tasks were used to inform computed muscle control (CMC) [4] simulations in OpenSim [5] to determine resultant JRFs at the glenohumeral joint. CMC tracked experimental kinematics of subjects pushing and pulling submaximal loads to 4 horizontal targets ($0^o$, $45^o$, $90^o$, and $135^o$) at a sagittal angle of $90^o$ and 3 sagittal targets ($20^o$, $90^o$, and $170^o$) at the $90^o$ horizontal target for a total of 6 independent task targets (Figure 1). Individualized musculoskeletal models were developed for each subject by scaling a previously developed and validated upper extremity musculoskeletal model [6] to individual joint strength and anthropometry.

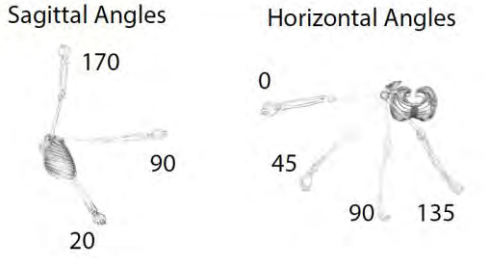


**Figure 1:** Task target location

Experimental electromyogram (EMG) recordings of surface muscles was used to inform on/off timing of the respective muscles, and thereby improve calculated activations for deep muscles. Furthermore, a penalty term was added to the static optimization stage of the CMC algorithm to constrain the resultant JRF to remain close to experimental limits of glenohumeral stability to prevent theoretical subluxation [7,8]. Differences in stability index, the ratio of transverse to compressive joint reaction forces at the glenohumeral joint, were analyzed across task direction and task target using a two-way ANOVA ($\alpha = 0.05$). If an interaction was present, simple main effects test was performed at each factor level.

## RESULTS AND DISCUSSION

An interaction between task target and task direction was present ($p=0.0037$). Pulling stability index was more spatially dependent than pushing (Figures 2 and 3). However, pushing was significantly less stable than pulling for all task targets ($p<0.001$) except for the sagittal target of $20^o$ ($p=0.1113$) (Figure 3).

Pushing was found to result in less stable joint reaction forces, which agrees with previous studies [2,3]. However, the results suggest that there are limited stability benefits to optimizing push task location. Greater stability benefits would be seen by converting push task to pull tasks where possible

since pulling, except from the low target, was inherently more stable than pushing. Workspaces involving pulling tasks, however, could benefit from optimizing task location, mainly by avoiding placing pull tasks at low targets. Placing pulling tasks at more centrally located targets along the horizontal plane improves task stability.

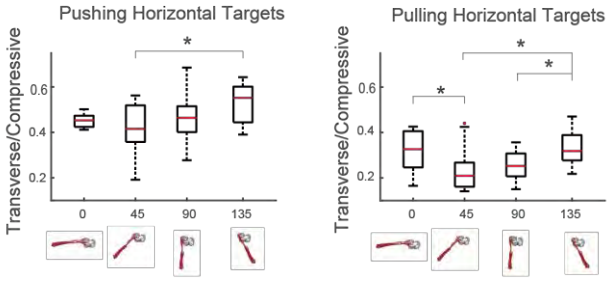


**Figure 2:** Stability index (transverse/compressive JRF components) across horizontal targets

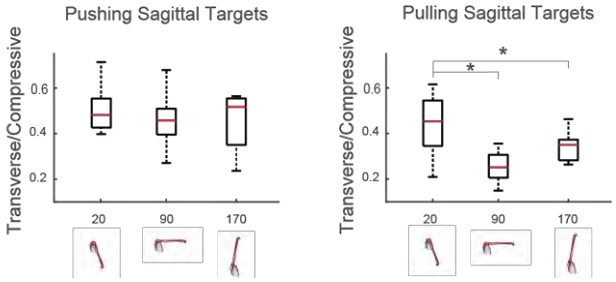


**Figure 3:** Stability index (transverse/compressive JRF components) across sagittal targets

Inherent task stability may influence muscle demand at the glenohumeral joint. Task targets identified as less stable in this study (i.e 20° for pulling and 135° for pushing) were reported to be significantly more demanding than other task targets [9]. Stabilization of the glenohumeral joint depends on active contributions of muscles, and this increase in demand may, in part, be due to an increased need to control the direction of the resultant joint reaction force.

One limitation of this research is that the kinematics of the handle in the experiment were not recorded. The direction of the applied loads was approximated from initial and final position of the hand's center of mass. Furthermore, strength data was only collected for shoulder abduction and elbow flexion, so strength scaling was limited to these measurements.

## CONCLUSIONS

The primary findings have possible implications for arm function throughout the workspace:

1. Pushing places the glenohumeral joint at increased risk for instability; however, the stability index for pushing is similar across targets. Therefore, larger stability benefits may be seen from converting tasks like lever operation from push tasks to pull tasks rather than optimizing task layout.
2. Inherent glenohumeral stability may contribute to increased task demand. Additional work is needed to fully understand to what degree these features are linked.

## REFERENCES


1. Lippitt and Matsen. *Clin Orthop Relat Res*, **291,** 20-28,1993.
2. Marchi et al. *Med Biol Eng Comput,* **52(3)**, 251-6, 2014.
3. Nimbarte et al. *Appl Ergon,* **44(5)**, 841-9, 2013.
4. Thelen et al. *J Biomech,* **36(3)**, 321-8, 2003.
5. Delp et al. *IEEE Trans Biomed Eng,* **54**, 1940-1950, 2007.
6. Saul et al. *Comput Methos Biomech Biomed Engin* **18(3)**, 1445-58, 2015.
7. Dickerson et al. *Comput Methos Biomech Biomed Engin* **10(6)**, 389-400, 2007.
8. Halder et al. *J Bone Joint Surg* **83(7),** 1062-1069, 2001.
9. McFarland et al. *Proceedings of ASB'17,* Boulder, CO, USA, 2017.


## ACKNOWLEDGEMENTS


We would like to acknowledge CFD Research Corporation for funding and Alexander Brynildsen and Lauren Levine for their assistance in post-processing kinematic data.

# MUSCULOSKELETAL MODEL-BASED CONTROL PERFORMANCE IS CONSISTENT ACROSS STATIC UPPER LIMB POSTURES

[1,2,3] Dustin L. Crouch, [2,3] Lizhi Pan, [3] William Filer, [2] Jonathan W. Stallings, and [2,3] He (Helen) Huang

[1] University of Tennessee, Knoxville, TN, USA
[2] North Carolina State University, Raleigh, NC, USA
[2] University of North Carolina at Chapel Hill, Chapel Hill, NC, USA
email: dustin.crouch@utk.edu

## INTRODUCTION

Electromyograms (EMG) are commonly used to estimate movement intent for control of human-machine interfaces (HMIs), such as prosthetic limbs. Emergent algorithms that aim to restore more life-like control can estimate simultaneous and independent movements across multiple joints [e.g. 1]. These algorithms typically require that each EMG is associated with only one primary biomechanical function (e.g. wrist extension). Recording such EMG is challenging in some HMI applications. For instance, EMG is susceptible to crosstalk when muscles are close to one another and overlapping (as in the proximal forearm of people with transradial amputation) and when it is recorded using surface electrodes (currently the only clinically-approved method for recording EMG for prosthesis control) [2]. Limb posture changes may also shift the location of surface electrodes relative to the underlying muscles and reduce the functional specificity of EMG [3]. We previously developed an EMG-driven, musculoskeletal model-based control algorithm that estimates simultaneous wrist and hand movements [4]. Using our algorithm, we conducted two studies to preliminarily evaluate the consistency of subjects' performance of a real-time control task across different limb postures and the extent to which performance could be improved with EMG processing and recording methods expected to provide more function-specific EMG.

## METHODS

*Musculoskeletal Model-Based Controller.* Our 2-degree-of-freedom (wrist and metacarpophalangeal (MCP) flexion/extension) model with four virtual muscles [4] was implemented for real-time EMG-driven control in MATLAB, as previously described [5]. Briefly, EMG were recorded from four forearm muscles that primarily contribute to wrist and/or MCP movement. EMG data were smoothed and normalized by EMG collected during maximum voluntary contractions (EMG-MVC) to estimate muscle activation state (0 = inactive, 1 = maximally active). Activations were applied to the virtual muscles during a forward dynamics simulation to estimate joint kinematics for real-time control of a 2-segment planar virtual hand on a video monitor.

*Real-Time Virtual Control Task.* In each trial, subjects attempted to move the virtual hand to each of four different target hand postures (Fig.1A) in a randomized order. For each target, subjects were first required to move both joints of the virtual hand to within 8° of a resting (relaxed) posture for 0.25 consecutive seconds, then to within 5° of the target posture for 0.5 consecutive seconds. We computed three task performance measures: task duration (**TD**), normalized path length (**NPL**, path length divided by minimum path length, in joint angle space), and number of overshoots (**NO**, overshoot= virtual hand moved in then out of target range).

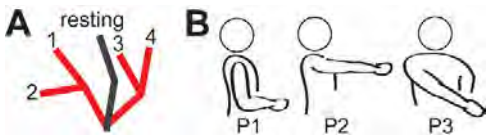


**Figure 1**: (A) Hand posture targets. (B) Static upper limb postures in which virtual task was performed.

*Study 1: EMG processing (normalization) method:* Seven able-bodied subjects (6 male, ages 21-32 years) gave their informed consent to participate. In each of 4 blocks of trials (12 trials per block), 4 trials were performed in each of 3 static upper limb postures in a randomized order: neutral arm with elbow at 90° flexion (P1), forward reach (P2), and contralateral reach (P3) (Fig.1B). Subjects assumed a neutral (F1) and pronated (F2) forearm posture in blocks 1/3 and 2/4, respectively. EMG were recorded using surface electrodes (sEMG). In blocks 1/2, EMG were normalized by EMG-MVC recorded in P1F1 (p1MVC); in blocks 3/4, EMG

were normalized by EMG-MVC recorded in the tested posture (psMVC). We performed a 3-way ANOVA to determine the effect of factors "upper limb posture", "forearm posture", and "EMG normalization method" on task performance.

*Study 2: EMG recording method:* Four able-bodied subjects from Study 1 (3 male, ages 21-25 years) and one transradial amputee (female, age 23) gave their informed consent to participate. In two sessions, EMG were recorded using either sEMG or fine-wire intramuscular electrodes (iEMG). iEMG were placed with ultrasound guidance in approximately the same muscles from which sEMG were recorded. For each electrode type, subjects performed 4 virtual task trials in each of 2 forearm postures (F1 and F2) in a randomized order. The amputee, unable to pronate the residual forearm, only performed trials in F1. We compared task performance between sEMG and iEMG trials using a Generalized Linear Mixed Model.

## RESULTS AND DISCUSSION

*Study 1*. TD (p=.005) and NPL (p=0.019) were statistically significantly worse (i.e. higher) in F2 than in F1; all other differences were not statistically significant (p>0.05). Notably, normalizing by psMVC, which was expected to improve the accuracy of computed muscle activation states, did not significantly improve task performance compared to trials in which EMG was only normalized by p1MVC (Fig.2). Analysis of EMG (not shown) indicated that subjects adapted their contraction effort to overcome differences in EMG magnitude across postures.

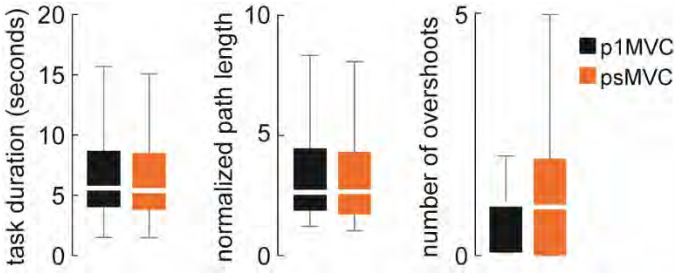


**Figure 2**: Box plot comparison of task performance measures between the two EMG-normalization conditions for able-bodied subjects (Study 1).

*Study 2.* There was a trend of more consistent, but not better, values of NPL with iEMG than sEMG (Fig.3). However, there was no statistically significant effect of electrode type or forearm posture (p>0.05). Qualitatively, for the subject with transradial amputation, all three task performance measures were worse with iEMG than sEMG.

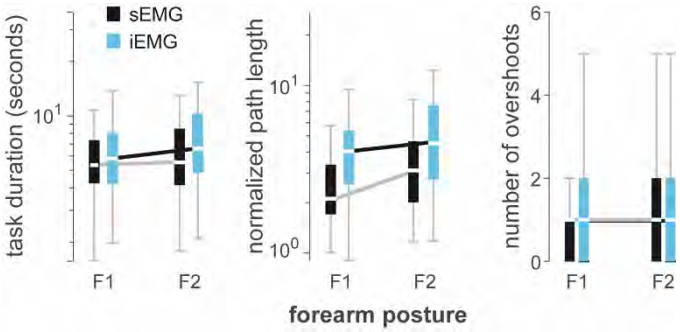


**Figure 3**: Box plot comparison of task performance measures between electrode type and between forearm postures for able-bodied subjects (Study 2).

## CONCLUSIONS

Our results suggest that sEMG and normalizing EMG to MVC from only one posture may be sufficient for providing reliable control of 2 degrees of freedom. This was surprising since both normalizing EMG by psMVC and iEMG recording were expected to provide better function-specific EMG and, thus, enable better real-time control performance. Some limitations of our study were the small sample size (only 1 amputee) and that testing conditions differed from those of real-world tasks (no physical prosthesis/socket, virtual tasks performed in static postures). Some subjects also verbally reported that iEMG felt unusual and/or uncomfortable, which may have confounded the effect of iEMG signal quality on task performance. Our results motivate future work to further evaluate our algorithm's potential to enable more natural control of prosthetic hands and other EMG-driven HMIs.

## REFERENCES

1. Smith et al. *IEEE Trans BME*, 63(4),2016.
2. Mogk & Kier. *J Electromyog Kinesio*, 13(1),2003.
3. Fougner et al. *IEEE TNSRE*, 19(6),2011.
4. Crouch & Huang. *J Biomech*, 49(16),2016.
5. Crouch & Huang. *J Neural Eng*, 14,2017.

## ACKNOWLEDGEMENTS

DARPA (N66001-16-2-4052), NSF (1527202, 1637892), DHHS/NIDILRR (90IF0064), DOD (W81XWH-15-C-0125, W81XWH-15-1-0407).

# WALKING BIOMECHANICS IN INDIVIDUALS WITH KNEE OSTEOARTHRITIS AFTER QUADRICEPS STRENGTHING

[1]Hope C. Davis, [2]Brittney A. Luc-Harkey, [1]J. Troy Blackburn, [1]Brian Pietrosimone

[1]University of North Carolina at Chapel Hill, Chapel Hill, NC, USA
[2]Brigham and Women's Hospital, Boston, MA, USA
davishc@live.unc.edu

## INTRODUCTION

Altered knee sagittal plane kinetics during walking are associated with worse pain outcomes in individuals with knee osteoarthritis (KOA) [1]. It is hypothesized that knee sagittal plane kinetics are influenced, in part, by quadriceps weakness [2]. Therefore, it is plausible that improving quadriceps strength may alter gait biomechanics. The primary purpose was to determine the association between baseline quadriceps strength and walking gait biomechanics linked to KOA onset and progression. The secondary purpose was to determine if individuals who increased quadriceps strength following 4-weeks of physical therapy (responders) demonstrated changes in gait biomechanics compared to individuals who did not increase quadriceps strength (non-responders).

## METHODS

*Physical Therapy for Knee Osteoarthritis*
53 individuals with radiographic and symptomatic KOA (Kellgren-Lawrence grade 2-4, 47% female, 62.3±7.1 years, BMI = 28.5±3.9 kg/m$^2$) were enrolled in 10 sessions of supervised, progressive lower extremity strengthening directed by a licensed physical therapist over a 28-day period.

*Quadriceps Strength*
Maximum isometric quadriceps strength was measured on the involved limb (with bilateral KOA, the involved limb was defined as the more symptomatic limb) using a dynamometer at baseline and following the 4-week physical therapy protocol. 3-5 maximal strength practice trials were conducted to determine a target torque threshold. Then 2 maximal effort trials were conducted where participants were instructed to straighten their knee as fast as possible to reach or surpass the target torque threshold. Quadriceps strength was defined as peak torque and normalized to body mass (Nm/kg). The minimal detectable change (MDC) of quadriceps strength was calculated using the standard error of measurement and intraclass correlation coefficient from the baseline quadriceps strength measurements [3]. Individuals who increased quadriceps strength by ≥0.31 Nm/kg were classified as strength responders; those who did not increase by this amount were classified as non-responders for the secondary analysis.

*Walking Gait Biomechanics*
Participants were outfitted with retroreflective markers and walked at a self-selected comfortable speed down a 6m walkway that contained 2 staggered, embedded Bertec force plates and a 10-camera three-dimensional motion capture system (Vicon Nexus). 5 trials were collected where the participant walked at a pace within 5% of the average speed determined during previous practice trials. Vertical ground reaction force (vGRF), knee flexion angle, and internal knee extension moment were time-normalized to percent of stance phase (heel-strike to toe-off) using linear interpolation techniques. Moments were normalized to the product of body weight (BW) and height (m), and vGRF was normalized to BW. Peak vGRF, knee flexion displacement, peak knee flexion angle, and peak internal knee extension moment (a larger negative value = greater moment) were identified during the first 50% of the stance phase. Ensemble average waveforms were created by averaging the waveforms of each trial for each participant.

*Statistical Analysis*
For the primary aim, linear regression analyses were conducted to determine associations between baseline quadriceps strength and biomechanical variables after accounting for walking speed as a

covariate ($\Delta R^2$). For the secondary aim, one-way ANCOVAs were conducted (percent change in walking speed from baseline to 4-weeks as the covariate) to determine differences between each biomechanical variable following 4-weeks of physical therapy between strength responders and non-responders. Next, ensemble average waveforms with 95% confidence intervals (CI) were plotted throughout the stance phase for responders and non-responders, and time points where 95% CI did not overlap were considered statistically different.

## RESULTS

There were no differences in demographics between responders (n=21) and non-responders (n=32). Greater peak vGRF (R = 0.37 $\Delta R^2$ = 0.08, p=0.02), peak knee flexion angle (R = 0.24, $\Delta R^2$ = 0.12, p=0.01), and peak internal knee extension moment (R = 0.12, $\Delta R^2$ = 0.08, p=0.04) all significantly associated with greater quadriceps strength after accounting for walking speed at baseline while knee flexion displacement (R = 0.11, $\Delta R^2$ = 0.06, p=0.07) did not. Between strength responders and non-responders, there were no significant differences in the percent change of any biomechanical variable from baseline to 4-weeks (p-values ranged from 0.31 to 0.52). Visual examination of ensemble average waveforms with 95% confidence intervals between responders and non-responders showed no significant differences in any portion of the stance phase for any biomechanical variable (Figure 1).

## DISCUSSION

Greater quadriceps strength associated with greater biomechanical variables at baseline; yet there were no differences in walking gait biomechanics between responders and non-responders to the strength intervention at either time point. Quadriceps strengthening may not be a mechanism directly responsible for an acute change in walking gait biomechanics in individuals with KOA. Future studies should consider directly targeting gait biomechanics with specific interventions to optimize gait in individuals with KOA, as quadriceps strengthening alone may not sufficiently influence adaptations in gait biomechanics.

## REFERENCES


1. O'Connell et al. *Clin Biomech*. 31:40-6. 2016.
2. Murray et al. *Clin Biomech*. 30(10):1140-5. 2015.
3. Harkey et al. *Gait Posture*. 59:128-33, 2018.


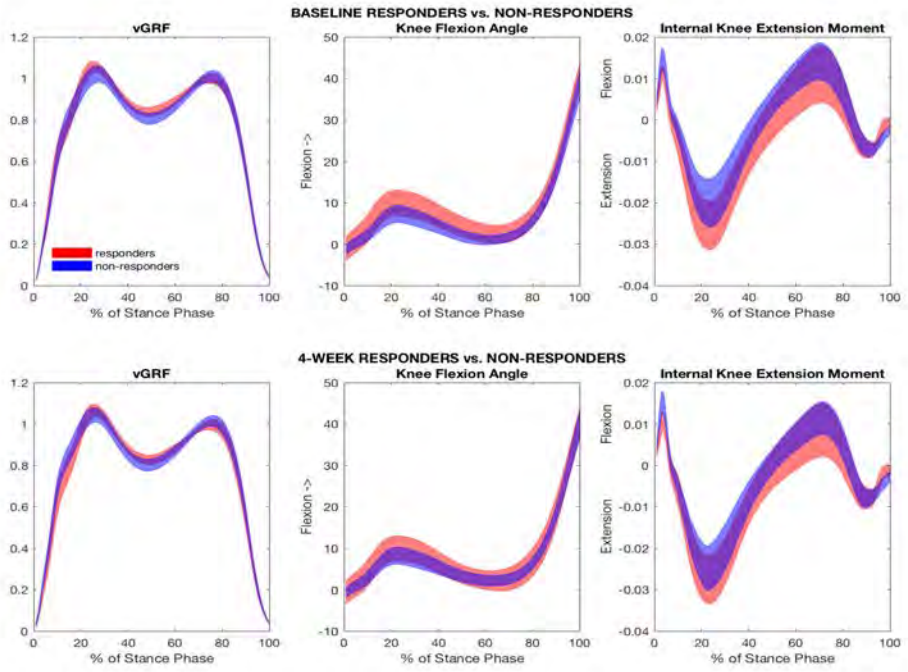


Figure 1. Ensemble average waveforms of vGRF, knee flexion angle and internal knee extension moment in individuals with KOA at baseline and 4-weeks following physical therapy.

# EFFECT OF BRACHIAL PLEXUS BIRTH INJURY LOCATION ON ALTERED GLENOHUMERAL MICROSTRUCTURE

[1,2] Emily B. Fawcett, [1]Nikhil N. Dixit, [1,2]Carolyn M. McCormick, [1,2]Ted A. Bateman, [1]Katherine R. Saul, and [1,2]Jacqueline H. Cole

[1] North Carolina State University, Raleigh, NC, USA
[2] University of North Carolina, Chapel Hill, NC, USA
email: ebfawcet@ncsu.edu, web1: http://www4.ncsu.edu/~ksaul/, web2: http://oml.web.unc.edu/

## INTRODUCTION

Brachial plexus birth injury (BPBI) is the most common nerve injury in children, causing muscle paralysis and ultimately leading to joint deformities and lifelong impairment of arm function in up to 30% of these children [1]. The injury is known to cause both muscle weakness and gross morphologic changes in the glenohumeral joint [2]. However, little is known about the underlying microstructure of both bone and muscle and how that correlates to the gross morphologic changes, including how it differs due to injury location along the nerve. Postural deformity is more severe with injuries occurring distal to the dorsal root ganglion (postganglionic) rather than proximal (preganglionic) [3]. This study uses unique rodent models of both injuries to improve understanding of factors contributing to glenohumeral joint deformities with BPBI.

The purpose of the study is to examine microstructural abnormalities in the bones surrounding the glenohumeral joint following BPBI and the impact of nerve injury location on the severity of these changes. Findings will help elucidate the differential progression of preganglionic and postganglionic injuries, a key first step to develop more effective treatments for children with BPBI.

## METHODS

All animal work was performed under an approved IACUC protocol. Male and female Sprague-Dawley rat pups were separated into three groups. The postganglionic neurectomy group (n=8) underwent C5 and C6 nerve root excision distal to the dorsal root ganglion [4]. The preganglionic neurectomy group (n=14) underwent C5 and C6 nerve root excision proximal to the dorsal root ganglion [5]. The sham control group (n=8) underwent sham surgery without nerve injury. Interventions were performed at postnatal day 3-5 on one side (affected) with the contralateral (unaffected) side serving as an additional control. At 8 weeks after surgery rats were sacrificed, and bones (humerus, scapula)were harvested from both affected and unaffected sides.

Bone microstructure was assessed in the distal scapula and proximal humerus using micro-computed tomography (micro-CT) (μCT 80, SCANCO Medical). Scans were reconstructed using a 10-μm isotropic voxel size, reoriented along anatomical planes, and calibrated for bone mineral density. Several volumes of interest (Fig. 1) were evaluated for standard trabecular bone metrics, including bone volume fraction (BV/TV), trabecular number (Tb.N), thickness (Tb.Th), and separation (Tb.Sp), and connectivity density (Conn.D). Analyses are ongoing, and a subset of data is presented here. Group comparisons were made on affected/ unaffected ratios using one-way ANOVA with Tukey's posthoc tests (α=0.05). The relationship between microstructural changes and

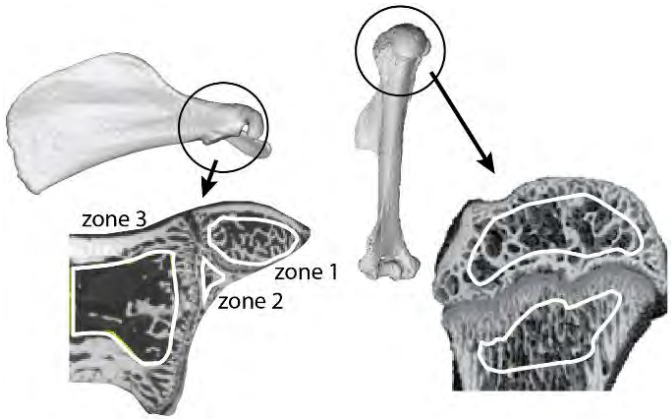


**Figure 1:** Micro-CT volumes of interest for the scapula (left) and humerus (right).

previously measured macrostructural changes in these animals will be examined with multivariate linear regressions (SAS).

## RESULTS AND DISCUSSION

Trabecular bone microstructure in the scapular zone 3 region was significantly deteriorated in rats with postganglionic neurectomy compared with sham (Fig. 2). Bone volume fraction in the affected limb (relative to unaffected) was reduced more for the postganglionic neurectomy group than sham (-20.5%, p=0.0014). The same was true for trabecular number (-20.1%, p<0.0001) and connectivity density (-18.2%, p=0.0061). Relative trabecular separation was increased for postganglionic compared to sham (+34.8%, p<0.0001). The preganglionic group (n=2 preliminary data) also showed deficits in trabecular microstructure similar those observed in the postganglionic group.

We previously found, in these same groups of rats, macrostructural differences between the post- and preganglionic groups [6]. In particular, the glenoid inclination angle was significantly reduced in the postganglionic but not in the preganglionic group. These disparate effects with injury location for macrostructural (different pre- vs. postganglionic) and microstructural (similar pre- vs. postganglionic) properties suggests different drivers for these changes in the scapula following BPBI that warrants further study.

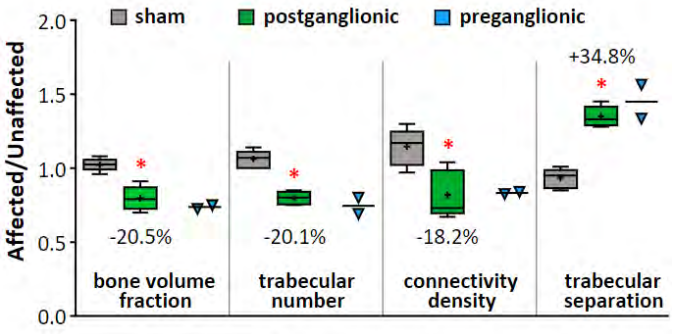


**Figure 2**: Compared to sham, postganglionic injury was associated with degenerated trabecular bone in scapula zone 3. Preganglionic rats (n=2) had similar changes compared to the sham group.
*p<0.05. + mean value.

## CONCLUSIONS

Our work shows substantial losses in scapular trabecular bone within 8 weeks of neonatal post-ganglionic injury, and a trend for losses in preganglionic injury, relative to sham. Specifically, the trabeculae were fewer, less connected, and more sparsely arranged following neurectomy. Most notably, this study will provide new information on how bone microstructural changes correlate with the development of glenohumeral deformities following BPBI, and how injury location may modulate these relationships.

These results are limited by a small sample size for the preganglionic injury, but data analysis is ongoing. The current work also focuses only on changes in bone tissue; as part of a larger study we are also looking at parallel changes in muscle microstructure (morphology and fibrosis), as well as underlying cellular crosstalk between muscle and bone, to elucidate mechanisms contributing to the tissue- and joint-level changes observed post-injury. This knowledge will help guide future work in evidence-based treatment planning to improve the current wait-and-see approach used in clinical practice [7].

## REFERENCES

1. Pondaag W (2004) *Dev Med Child Neurol* 46:138.
2. Crouch DL (2015) *J Bone Joint Surg Am* 97:1264.
3. Al-Qattan MM (2003) *Ann Plast Surg* 51:257.
4. Li Z (2010) *J Bone Joint Surg Am* 92:2583.
5. Nikolaou S (2015) *J Hand Surg* 40:2007.
6. Dixit NN (2018) *Orthop Res Soc Annual Meeting*
7. Hale HB (2010) *J Hand Su*rg 35:322.

## ACKNOWLEDGMENTS

This study was funded by NIH R21HD088893. We thank Eric Livingston for micro-CT scanning.

# VISUOMOTOR ERROR AUGMENTATION AFFECTS MEDIOLATERAL HEAD AND TRUNK STABILIZATION DURING WALKING

Mu Qiao, Jackson T. Richards, and Jason R. Franz

University of North Carolina and North Carolina State University, Chapel Hill, NC, USA
Email: jrfranz@email.unc.edu, web: http://abl.bme.unc.edu

## INTRODUCTION

Humans regulate lateral balance in walking through coordinated adjustments between the continuous control of posture (*i.e.*, head and trunk stabilization) and the discrete (step-to-step) control of foot placement (*i.e.*, step width). These corrective adjustments strongly depend on the integration of reliable sensory feedback. Accordingly, walking balance is acutely susceptible to optical flow perturbations designed to elicit the visual perception of lateral imbalance. Specifically, in response to those perturbations, we recently discovered that head and trunk kinematics during walking instinctively synchronize (*i.e.*, entrain) to a broad range of driving frequencies of perceived mediolateral (ML) motion [1]. In that study, we speculated that this entrainment acted to minimize errors between the visual perception of motion and the actual motion of the head and trunk, thereby unifying visual with vestibular and somatosensory feedback. However, we lacked direct evidence that minimizing these 'visual prediction errors' was a control goal for head and trunk stabilization during human walking.

Therefore, we investigated the role of visual prediction errors in governing the control of mediolateral head and trunk position during human walking as a means to explain the acute postural response to optical flow perturbations. Specifically, we used a visuomotor error augmentation paradigm in which optical flow was synchronized to instantaneous head and trunk kinematics recorded via motion capture. We hypothesized that minimization of visual prediction errors, achievable during the task by reducing lateral head and trunk movement, is an important and instinctive feature governing walking balance control. The alternative hypothesis would be that visual feedback overrides other sensory modalities and is itself an independent control parameter in regulating head and trunk position. We also tested the hypotheses that the response to error-augmented optical flow would: (*i*) scale (*i.e.*, increase) with larger feedback gains and (*ii*) exhibit tuning via time-dependent adaptation following prolonged exposure.

## METHODS

Twelve subjects participated (8M/4F, age: 24.1±4.7 yrs, body mass: 73.3±13.0 kg; height: 176±9 cm, mean±S.D.). All subjects walked at their preferred walking speed (1.36±0.14 $m \cdot s^{-1}$) on an instrumented split-belt treadmill (Bertec Corp., Columbus, OH) while watching a speed-matched, virtual hallway rear-projected onto a semi-circular screen surrounding the treadmill (1.45 m radius × 2.54 m height, Fig. 1). A 3D motion capture system (Motion Analysis Corp., 100 Hz) recorded the trajectories of markers placed on subjects' pelvis, legs, and 7$^{th}$ cervical (C7) vertebra. In real-time, a Simulink® controller prescribed the mediolateral (ML) position of the virtual hallway for all trials based on the instantaneous ML position of subjects' C7 marker, which we selected as the highest point on the trunk that is not affected by head orientation. In some trials, we introduced errors between the visual perception of self-motion (via optical flow) and actual ML motion of head and trunk using a position gain, *G* (Fig. 1). Across different conditions, *G* took

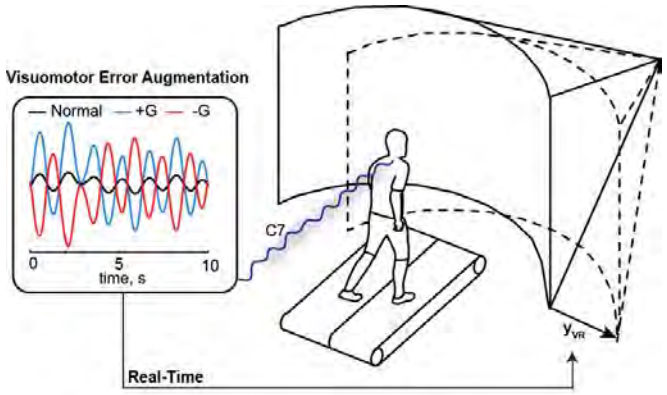


**Figure 1**. Subjects walked in a virtual environment with visuomotor error augmentation based on instantaneous measurements of their mediolateral (ML) C7 position.

4 values (±2.5 and ±5.0), the largest of which determined in pilot testing to ensure that the virtual hallway remained on the projection screen. Positive/negative values indicate the ML motion of the virtual hallway was in the same/opposite direction of the measured ML C7 motion. Subjects first walked for 1 min with the normal oncoming optical flow (G=0, baseline). Subjects then walked for 10 min with the error-augmented optical flow with one of the four gains. Each of these trials ended with 1 min of walking with the normal oncoming optical flow (G=0, post). Dependent variables included the step-to-step range of ML trunk motion (intra-step measure), and the root mean square (RMS) of ML trunk position (inter-step measure).

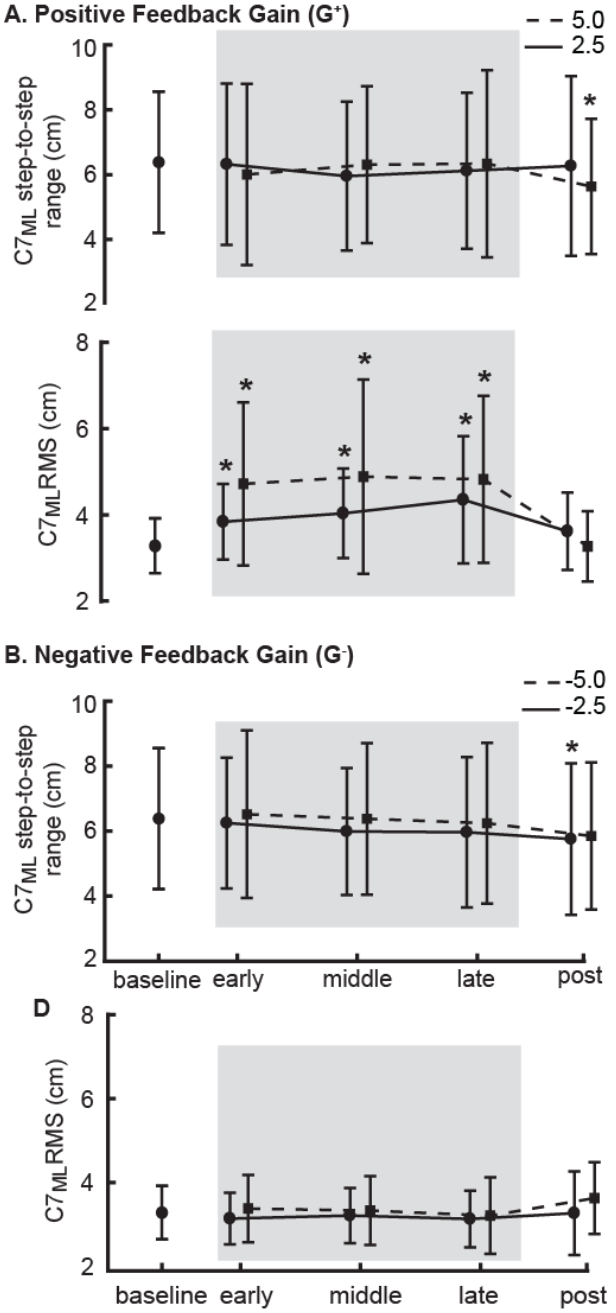


**Figure 2**. Intra- and inter-step mediolateral trunk motion from all steps across the protocol. Asterisks (*) indicate different from baseline ($p$<0.05).

## RESULTS AND DISCUSSION

In contrast to our hypothesis, neither intra- nor inter-step measures of ML trunk motion amplitude decreased in the presence of error-augmented optical flow (Fig. 2). Rather, larger positive visual prediction errors increased the RMS of ML trunk position – an effect that scaled in proportion to feedback gain amplitude (early vs. baseline, $p$<0.05, Fig. 2A). These early responses to error-augmented optical flow persisted with prolonged exposure; we found no significant effects of time (i.e., early, middle, late) on step-to-step ML trunk range of motion ($G^+$: p=0.856, $G^-$: p=0.124) nor the RMS of ML trunk motion ($G^+$: p=0.204, $G^-$: p=0.552) (Fig. 2). Following 'release' of error-augmented optical flow, the RMS of ML trunk position returned to baseline values within one minute. However, despite no apparent effects of time during exposure, the step-to-step trunk range of motion decreased significantly following exposure compared to baseline walking (-12% for G=+5.0, $p$=0.002, Fig. 2A; -10% for G=-2.5, $p$=0.002, Fig. 2B). Those after-effects were also accompanied by longer and wider steps, but only following walking with positive feedback gains.

## CONCLUSIONS

Subjects did not instinctively minimize errors between the visual perception of movement and actual movement of the head and trunk. Our results are instead more consistent with our alternative hypothesis – that visual feedback can override other sensory modalities and independently compel adjustments in head and trunk position. Our results also allude to a recalibration of head and trunk stabilization toward more tightly regulated postural control following exposure to error-augmented optical flow. Although this study focused on young adults, lasting reductions in ML postural sway evident in our data may have important implications for enhancing the integrity of walking balance control through training, for example in older adults.


## ACKNOWLEDGEMENTS

Funded by a grant from NIH (R56AG054797).


## REFERENCES


[1] Franz et al., IEEE TNSRE 2017: 25(8).

# Temporal response of muscle-bone deformities at the shoulder following brachial plexus birth injury

[1] Nikhil Dixit, [1,2] Jacqueline H. Cole, and [1]Katherine Saul

[1] North Carolina State University, NC, USA
[2] University of North Carolina-Chapel Hill, NC, USA
email: ndixit2@ncsu.edu

## INTRODUCTION

Brachial plexus birth injury (BPBI) is a traumatic perinatal neuromuscular injury causing muscle paralysis, shoulder contracture, and deformed growth of the scapula and humerus [1-3]. The resulting lifelong impairment greatly limits critical activities of daily living, such as eating and bathing. Almost nothing is known about the timing and mechanisms of changes in underlying bone and muscle structure following nerve injury occurring at birth to provide a foundation for clinical decision-making. As a result, there is currently no consensus on optimal timing or approach for therapy after injury [4], leading to inconsistent clinical outcomes. When the brachial plexus is injured in children outside of the neonatal period, there is limited contracture compared to BPBI, providing a unique opportunity to explore why the same injury in a similar period of rapid musculoskeletal growth avoids marked deformity.

Understanding the timing and mechanism of deformity initiation is essential for developing treatments that prevent bone and postural deformities from developing, rather than correcting deformity after formation. The objective of this work is to identify whether deformity is initiated first in muscle or bone by examining gross bone and muscle structure and contracture, and to explore how tissue response to injury depends on timing of injury.

## METHODS

The study protocol was approved by the NC State IACUC. We used an existing rat model of BPBI developed in our group [5]. Because contracture and bone deformity are known to depend clinically on whether the nerve injury is proximal or distal to the dorsal root ganglion [6], we explored these effects in models of both injuries. Nerve injuries were created under isoflurane anesthesia using standard aseptic technique [7]. For preganglionic neurectomy, the C5 and C6 nerve roots were excised proximal to the dorsal root ganglion, partially preserving afferent innervation and muscle spindle function [8], which produces nerve damage without marked postural shoulder contracture. For postganglionic neurectomy, the C5 and C6 nerve roots were excised distal to the dorsal root ganglion, resulting in nerve damage and associated increases in shoulder contracture.

The progression of shoulder deformity after neonatal injury was examined by intervention at postnatal day 4 (P4), and progression was examined using 3 timepoints (2, 4, and 5 weeks post injury). The effect of injury timing (neonatal vs. postnatal) was examined by using a 4-week postnatal injury age (P4wks). Rats were provided water and rat chow *ad libitum* and sacrificed at the respective timepoints via $CO_2$ asphyxiation. To assess changes in muscle and bone structure and deformity, we measured passive external rotation range of motion (ROM) to analyze shoulder contracture ($n_{preganglionic} = 16$, $n_{postganglionic} = 22$) [5], glenoid inclination angle using micro-computed tomography, and optimal muscle fiber length of biceps long head (BICLong) using a laser diffraction technique (P4 postganglionic: $n_{2wks} = 1$, $n_{4wks} = 4$ for glenoid inclination angle and 1 for BICLong fiber length, $n_{5wks} = 1$; P4 preganglionic: $n_{4wks} = 1$; P4wks: $n_{postganglionic} = 1$; $n_{preganglionic} = 1$) [7]. Due to challenges in the preganglionic procedure, we looked only at the 4-week post-injury timepoint. Measures in the affected limb were compared relative to those in the contralateral unaffected limb.

## RESULTS AND DISCUSSION

Our analyses of muscle and bone structure in rats following P4 pre- and postganglionic neurectomy support early changes to muscle and bone when

nerve injury is inflicted in the neonatal period (Figure 1, P4). Range of motion at 4 weeks post-neurectomy indicated more contracture in the postganglionic group compared to preganglionic group, consistent with previous studies [6]. Glenoid inclination measured at 2, 4, and 5 weeks tended to be more declined in the affected shoulder, with deformity values increasing with time for the postganglionic group. Biceps long head in the affected limb tended to be shorter than the contralateral limb at the same timepoints for postganglionic injury.

In contrast, analyses of bone and muscle following postganglionic neurectomy at P4wks showed that limited deformity to bone and muscle was observed when neurectomy occurred postnatally. Minimal changes to glenoid inclination and muscle length were observed at 2 and 4 weeks post-neurectomy (Figure 1, P4wks). Our results in rats are consistent with another study of the elbow following postganglionic injury in mice [9]. In that study, elbow contracture following postganglionic neurectomy at P4wks (n=17) was nearly absent, with no contractures more than 10°, and significantly lower ($p<0.001$) than in mice with neonatal postganglionic injury (n=42) [9], with elbow contractures up to 40°.

## CONCLUSIONS

Our preliminary work shows gross alterations in both muscle and bone by 4 weeks after neonatal injury in rats (~1 year in infants [7]), suggesting early tissue changes at odds with the wait-and-see approach in clinical practice [5]. The observed bone and muscle deformities due to a neonatal injury become more severe over time. However, severe deformities do not occur when the injury occurs postnatally. This study provides new information about the effect of time progression and timing of BPBI.

The current work is limited by a small sample size and limited time points for preganglionic injury; data collection is ongoing. Further, the current work identifies structural changes alone; ongoing work examines the underlying changes in metabolism, microstructure, and mechanics to explicate the observed macrostructural changes.

## REFERENCES


1. Hogendoorn (2010) *J Bone Joint Surg Am* 92:935.
2. Pearl (1998) *J Bone Joint Surg Am* 80:659.
3. Poyhia 2005) Pediatr Radiol 35:402.
4. Belzberg (2004) *J Neurosurg* 101:365.
5. Li (2008) *J Hand Surg* 33(3):308-12.
6. Al-Qattan (2003) *Ann Plast Surg* 51:257.
7. Crouch (2015) *J Bone Joint Surg Am* 97:1264.
8. Nikolaou (2015) *J Hand Surg* 40:2007.
9. Weekley (2012) *J Orthop Res* 30:1335.


## ACKNOWLEDGMENTS


The study was funded by NIH R21HD088893. Contributions were made by Eric Warren in muscle sarcomere length measurements and Dr. Ted Bateman and Eric Livingston in micro-CT scans.


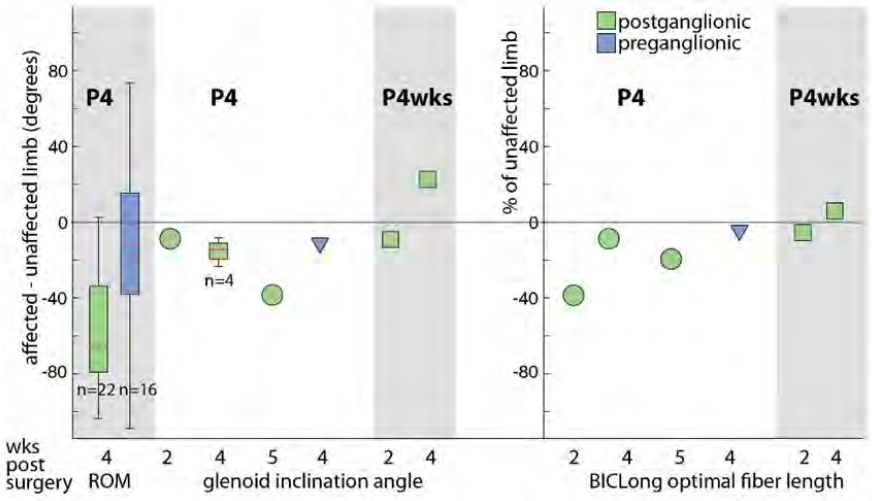


Figure 1: ROM, glenoid inclination angle, and biceps long head optimal fiber length for P4 and P4wks neurectomy at multiple timepoints. n=1 per timepoint unless noted.

# CHRONOLOGICAL COMPARISON OF WALKING GROUND REACTION FORCE IN INDIVIDUALS WITH ANTERIOR CRUCIATE LIGAMENT RECONSTRUCTION

[1]Matthew K. Seeley, [2]Christopher Johnston, [2]Steven J. Pfeiffer,
[2]Jeffrey T. Spang, [2]J. Troy Blackburn & [2]Brian G. Pietrosimone

[1] Brigham Young University, Provo, UT, USA
[2] University of North Carolina at Chapel Hill, Chapel Hill, NC, USA
email: matt_seeley@byu.edu

## INTRODUCTION

Vertical ground reaction force (vGRF) is a fundamental measure of external load transmitted to lower extremity joints, including the knee. Walking vGRF is linked to multiple indicators of knee cartilage health, including knee tissue metabolism and cartilage composition, and patient reported function following anterior cruciate ligament reconstruction (ACLR) [1]. Approximately 40% of ACLR patients report clinically relevant knee symptoms years after ACLR [2], and these symptoms are associated with aberrant movement biomechanics [3], which may influence the long-term health of knee joint tissue. The association, however, between persistent clinically relevant knee symptoms and aberrant biomechanics, post-ACLR, is unclear. The purpose of this project was to compare walking vGRF transmitted to the involved leg of clinically symptomatic and asymptomatic ACLR patients, at three clinically relevant time periods: 6-11, 12-24, and > 24 months post-ACLR. We hypothesized that, relative to the asymptomatic patients, symptomatic patients would exhibit decreased walking vGRF at 6-11 months post-ACLR, but increased vGRF at 12-24 and > 24 months post-ACLR.

## METHODS

vGRF were measured for 5 walking trials, for 128 post-ACLR patients (Table 1). All procedures were approved by the appropriate institutional review board before data collection. Patients were classified as clinically symptomatic or asymptomatic using the Knee Injury and Osteoarthritis Outcome Score, as previously defined [4]. Patient descriptors (Table 1) were compared, between groups, for each time, using *t* tests ($\alpha = 0.05$). Multiple 2 × 2 functional ANOVAs were used to evaluate effects of group (symptomatic and asymptomatic) and time post-ACLR (6-11 months, 12-24 months, and > 24 months) on walking vGRF. This functional statistical approach allowed for detection of statistical differences throughout stance, rather than only at certain discrete time points (e.g., peak vGRF). Estimates of pairwise comparison functions were plotted for the symptomatic and asymptomatic groups, for each of the three different time periods (Figures 1A-C), as well as 95% confidence intervals, to determine significant differences (Figures 1D-F); vGRF were considered to be statistically different when confidence intervals did not cross zero (Figures 1D-F).

**Table 1:** Descriptions of six different subgroups of ACLR patients included in this analysis.

| | 6-11 Months | |
|---|---|---|
| | Symptomatic | Asymptomatic |
| n (females) | 28 (16) | 24 (14) |
| Age (Years) | 22 ± 3 | 22 ± 4 |
| BMI (kg/m$^2$) | 24.9 ± 4.0 | 25.0 ± 4.0 |
| Gait Speed (m/s) | 1.23 ± 0.15 | 1.25 ± 0.13 |
| | 12-24 Months | |
| | Symptomatic | Asymptomatic |
| n (females) | 15 (11) | 15 (10) |
| Age (Years) | 20 ± 3 | 22 ± 4 |
| BMI (kg/m$^2$) | 23.4 ± 3.6 | 25.4 ± 4.2 |
| Gait Speed (m/s) | 1.22 ± 0.11 | 1.21 ± 0.14 |
| | >24 Months | |
| | Symptomatic | Asymptomatic |
| n (females) | 13 (13) | 33 (22) |
| Age (Years) | 19 ± 2 | 21 ± 2 |
| BMI (kg/m$^2$) | 24.2 ± 3.3 | 24.9 ± 4.5 |
| Gait Speed (m/s) | 1.31 ± 0.26 | 1.18 ± 0.19 |

## RESULTS AND DISCUSSION

None of the patient descriptors reported in Table 1 differed between the symptomatic and asymptomatic patients, for any of the time periods. For the 6-11 months time period, walking vGRF were less for the

symptomatic group, during most of the first and final third of stance, but greater during most of the middle third of stance (Figures 1A and 1D). Between-group differences diminished for the 12-24 months time period, and only existed between 5 and 8%, and 92 and 95% of stance (Figures 1B and 1E). Between-group differences also existed for the > 24 months time period, when walking vGRF were greater for the symptomatic group during most of the first and final third of stance, but less during most of the middle third of stance (Figures 1C and 1F). Although not presented here, between-time comparisons, for each group, indicated that the variation in between-group differences, across the three observed time periods, was due more to between-time differences for the symptomatic groups, while asymptomatic vGRF was similar between indiviudals at different time points.

It is possible that vGRF differences observed during the first year post-ACLR are due to kinesiophobia or inability to bear weight on the ACLR limb, while the latter differences (> 24 months) might be more related to inadequate lower-extremity muscular capacity to control the limb during gait. We further speculate that presently observed vGRF differences may reflect differences in knee joint loading patterns that are detrimental to joint tissue health at the knee. Additionally, it should be emphasized that this analysis involved 128 different ACLR patients, each at various times post-ACLR; a longitudinal study of the same symptomatic and asymptomatic patients, and associated biomechanics, is warranted.

## CONCLUSIONS

The present analyses indicate that symptomatic and asymptomatic ACLR patients utilize different loading patterns during walking, and that these differences vary depending upon time post-ACLR. Symptomatic ACLR patients appear to unload their affected leg, during the first year, post surgery; however, these abnormal loading patterns appear to reverse later in time, > 24 months post surgery.

## REFERENCES


1. Pietrosimone et al. *J Orthop Res.* 35(10), 2288-2297, 2017.
2. Wasserstein et al. *Osteoarthritis Cartilage.* 23(10), 1674-1684, 2016.
3. Pietrosimone et al. *J Orthop Res.* In Press.
4. Englund et al. *Arthritis Rheum.* 48(8), 2178-2187, 2003.


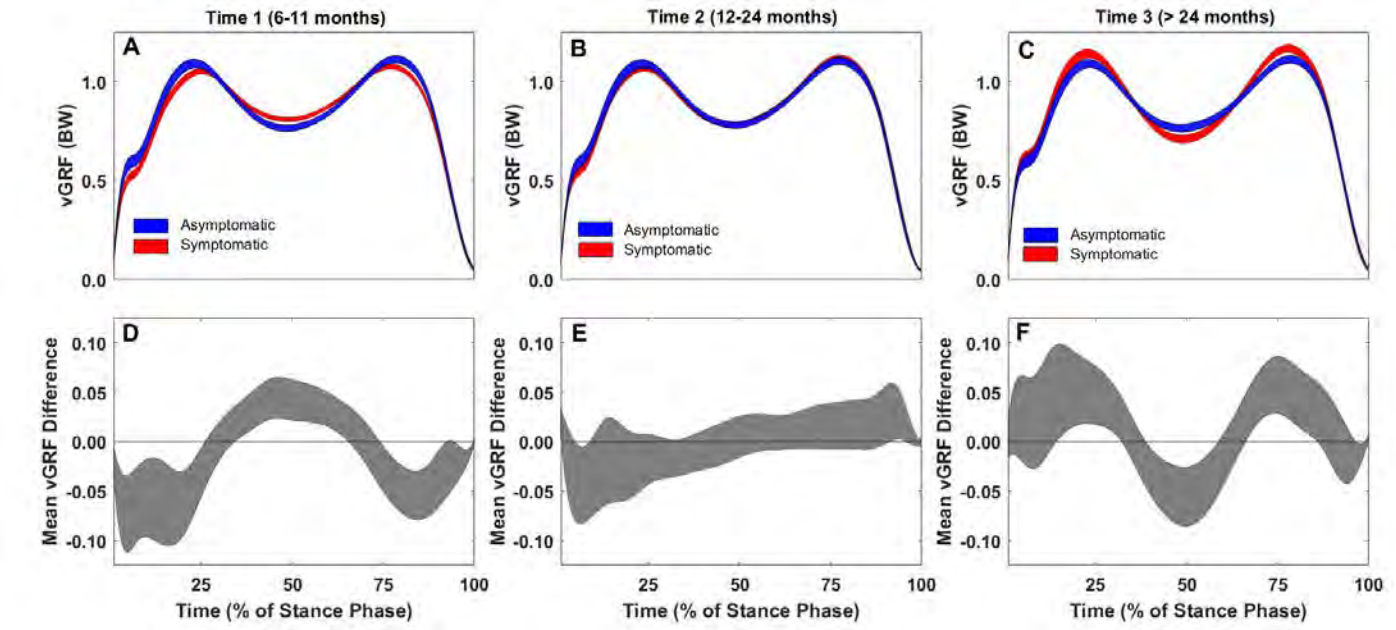


**Figure 1:** Mean walking vGRF for 128 different ACLR patients (A-C), at three different time periods, and the corresponding mean differences and estimated effect sizes (D-F). Relative to the asymptomatic patients, peak vGRF was usually less ($\alpha = 0.05$) for the symptomatic patients at 6-11 months, but greater at > 24 months (differences are indicated whenever the effect sizes did not overlap zero in D-F).

# GAIT ASYMMETRIES 6 MONTHS POST-ACLR ASSOCIATE WITH INTER-LIMB T1ρ RATIOS 12 MONTHS POST ACLR

[1]Steven J. Pfeiffer, [1]Jeffrey Spang, [1]Daniel Nissman, [1,2]David Lalush, [1]Kyle Wallace, [3]Matthew S. Harkey, [1]Laura Stanley, [4]Randy Schmitz, [1]Troy Blackburn, [1]Brian Pietrosimone

[1] University of North Carolina at Chapel Hill, Chapel Hill, NC, USA, [2] North Carolina State University, Raleigh, NC, USA, [3]Tufts Medical Center, Boston, MA, USA, [4]University of North Carolina at Greensboro, NC, USA. email: stevenpf@email.unc.edu

## INTRODUCTION

Individuals who sustain an anterior cruciate ligament injury and reconstruction (ACLR) are at heightened risk for posttraumatic knee osteoarthritis (PTOA).[1] The progression to PTOA following ACLR is theorized to result from an interaction between aberrant joint biomechanics during walking and deleterious biological changes to the knee cartilage.[2] Alterations in proteoglycan density within the cartilage matrix are hypothesized to be one of the initial cartilage changes that may be related to PTOA development.[3] T1ρ magnetic resonance imaging (MRI) relaxation times are sensitive to proteoglycan density changes and are elevated, indicating worse proteoglycan density, as early as one year post-ACLR.[4] The purpose of this study was to determine the associations between limb symmetry indices (LSI) for gait biomechanics measured six months post-ACLR and femoral T1ρ relaxation times twelve months post-ACLR. We hypothesized individuals with lesser loading of the ACLR limb six months following ACLR would demonstrate greater T1ρ MRI relaxation times on the ACLR limb twelve months following surgery.

## METHODS

Twenty-four individuals (50% female, 21.92 ± 3.61 years old, 178.13 ± 11.30 cm, 75.35 ± 12.60 kg) with a unilateral bone-patellar-bone autograft ACLR participated in this study. Walking biomechanics [peak vertical ground reaction force (vGRF), vGRF loading rate (vGRF-LR), and peak internal knee extension moment (KEM)] were extracted from the first 50% of stance phase in both limbs during five trials of walking at self-selected speed six months following ACLR. LSI were used to normalize the biomechanical outcomes of the ACLR limb to the uninjured limb (ACLR Limb / Uninjured limb). Peak vGRF (BW) and vGRF-LR (BW/s) were normalized to body weight. vGRF-LR was calculated as the peak of the first derivative of the force-time curve. KEM was calculated using an inverse dynamics approach and was normalized to the product of body weight and height (BW*m). KEM was expressed as an internal moment and a negative value.

A 3-Tesla scanner was used to acquire images following 30 minutes of unloading the knee joint. T1ρ relaxation times were calculated (Figure 1) for the medial and lateral femoral condyles (MFC & LFC) using a five-image sequence created with a MatLab program with the following equation: $S(TSL) = S0 \exp(-TSL/T1\rho)$ where TSL is the duration of the spin-lock time, S0 is signal intensity when TSL equals zero, S corresponds to signal intensity, and T1ρ is the T1 relaxation time in the rotating frame. Prior to segmentation, affine and non-rigid deformable registration techniques were utilized to align the ACLR limb to the uninjured limb. The weight bearing portions of the cartilage of the MFC and LFC was manually segmented into posterior, central, and anterior regions of interest (ROI) based on the location of the meniscus in the sagittal plane.[5] Inter-limb T1ρ relaxation time ratios (T1ρ ILR = ACLR limb T1ρ / uninjured limb T1ρ) were calculated for each ROI.

**Figure 1:** Representative map of T1ρ relaxation times of an ACLR (L) and contralateral (R) knee.

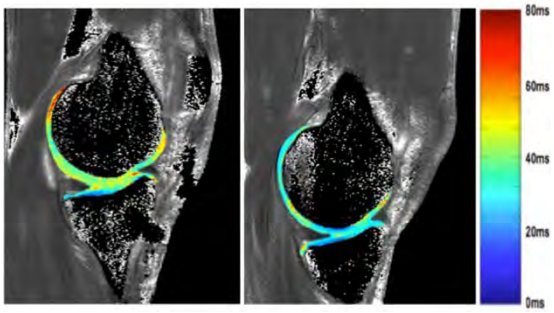

Separate, stepwise linear regressions were used to determine the unique associations between knee biomechanical outcomes and ILR for each ROI ($\Delta R^2$, $\beta$, $P \leq 0.05$). Self-selected gait speed and the presence of a meniscal injury may influence T1ρ MRI relaxation times following ACLR. Therefore, these variables were entered into the regression model first followed by the biomechanical variable of interest. The presence of a medial or lateral meniscal injury was entered when specifically evaluating ILR of cartilage in either the medial or lateral compartment, respectively.

## RESULTS

Lesser peak vGRF LSI six months following ACLR significantly associated with greater Posterior-LFC T1ρ ILR ($\Delta R^2$=0.20, $\beta$=-0.48, P=0.04) twelve months following ACLR. Similarly, lesser peak vGRF-LR LSI six months following ACLR significantly associated with greater Posterior-MFC T1ρ ILR ($\Delta R^2$=0.19, $\beta$=-0.45, P=0.05) twelve months following ACLR. Additionally, lesser peak KEM LSI six months following ACLR significantly associated with greater Central-MFC T1ρ ILR ($\Delta R^2$=0.19, $\beta$=0.46, P=0.04) twelve months following ACLR.

## DISCUSSION

Consistent with our hypothesis, individuals with lesser peak vGRF LSI, vGRF-LR LSI, and peak internal KEM LSI during walking six months following ACLR, demonstrated greater T1ρ ILR in the medial and lateral femoral condyles. These findings suggest that lesser mechanical loading of the ACLR limb compared to the uninjured limb early (i.e. 6 months) following ACLR may be related to deleterious changes in proteoglycan density of the ACLR limb compared to the uninjured limb at a later time point following ACLR (i.e. 12 months).

Both excessive and insufficient mechanical loading of the knee can lead to breakdown of tibiofemoral cartilage within the joint. Recent evidence[6,7] has demonstrated that excessive mechanical loading during walking early following ACLR associates with increased T1ρ relaxation times at early and later time points following ACLR. The findings of the current study are contrary to these studies but are consistent with previous findings demonstrating that lesser mechanical loading during walking following ACLR associates with changes in cartilage metabolism,[8] structure,[9] and future PTOA development.[10] Future work is needed to further understand the association between joint loading and deleterious changes to joint tissue metabolism following knee joint injury in order to develop interventions to optimally load the joint for the purpose of improving long-term joint health.

## CONCLUSIONS

The findings of the current study illustrate that mechanical loading, specifically lesser loading, between limbs during walking early following ACLR may be related to deleterious changes of the cartilage matrix at later time points following ACLR, which may be related to the development of future PTOA. These findings illustrate the need for establishing optimal mechanical loading patterns during walking early in the rehabilitation process.

## REFERENCES


1. Luc B, et al. *Journal of Athletic Training*. 2014;49(6):806-819.
2. Andriacchi TP, et al. *Annals of Biomedical Engineering*. 2015;43(2):376-387.
3. Regatte RR, et. al. *Academic Radiology*. 2002;9(12):1388-1394.
4. Regatte RR, et al. *Journal of Magnetic Resonance Imaging*. 2006;23(4):547-553.
5. Pfeiffer S, et al. *Arthritis Care and Research (Hoboken)*. 2017.
6. Kumar D, et al. *American Journal of Sports Medicine*. 2018;46(2):378-387.
7. Teng HL, et al. *American Journal of Sports Medicine*. 2017: 45(14): 3262–3271.
8. Pietrosimone B, et al. *Journal of Orthopedic Research*. 2017. 35(10): 2288–2297
9. Saxby DJ, et al. *Orthopedic Journal of Sports Medicine*. 2017;5(8).
10. Wellsandt E, et al. American Journal of Sports Medicine. 2016;44(1):143-151.

# OLDER ADULTS REVERSE THEIR DISTAL-TO-PROXIMAL REDISTRIBUTION USING BIOFEEDBACK

Michael G. Browne, Sarah N. Fickey, and Jason R. Franz

University of North Carolina at Chapel Hill and North Carolina State University, Raleigh, NC, USA
email: mgbrowne@email.unc.edu, web: http://abl.bme.unc.edu

## INTRODUCTION

Compared to young adults, older adults walk slower and with a characteristic decrease in push-off intensity. This decreased push-off intensity stems from large reductions in mechanical power generated by the plantarflexor muscles (i.e. ankle power, $P_A$) and propulsive ground reaction forces generated during push-off ($F_P$) [1]. Seemingly in response to this decreased push-off intensity, older adults also rely more on positive mechanical power generated by the hip musculature. This phenomenon, known as the distal-to-proximal redistribution [2], may also contribute to increased metabolic energy costs during walking in older adults [3]. Conventional resistance training for improved mobility in older adults successfully improves maximal muscle strength and fast walking speed (FWS) but has minimal functional impact on habitual walking performance (i.e. preferred walking speed; PWS) or gait biomechanics (e.g., mechanical power generation).

Rehabilitative approaches that go beyond resistance training alone are needed, toward more direct means to elicit favorable biomechanical adaptations during habitual speed walking. As an important first step, we previously attempted to enhance push-off intensity in older adults using biofeedback to increase propulsive forces. While effective - older adults increased $F_P$ with potentially favorable reductions in hip flexor power generation [4] – we were surprised to observe no concomitant increase in $P_A$. However, older adults can increase $P_A$ in order to walk faster or uphill, revealing a translationally important gap in our understanding. Motivated by these findings, we tested here the primarily hypothesis that real-time ankle power biofeedback during walking can directly increase $P_A$ in older adults. We also hypothesized that doing so would: (*i*) alleviate mechanical power demands at the hip and (*ii*) increase preferred but not fast walking speed.

## METHODS

10 healthy older adults (mean±SD; age: 74.8±5.4 years, 3 males/7 females) participated in this study. We first assessed subjects' PWS (1.28±0.20 m/s) and FWS (1.79±0.20 m/s) using an instrumented walkway. Subjects then walked normally for 1-min on a dual-belt instrumented treadmill at their PWS. A custom Matlab script running a surrogate inverse dynamic model of the lower legs and feet estimated bilateral step-by-step $P_A$. Subjects walked again for 1-min each while watching a screen with visual biofeedback of their instantaneous $P_A$ and targeting increases of +10% and +20% of normal (Fig. 1A). For all trials, a motion capture system recorded the

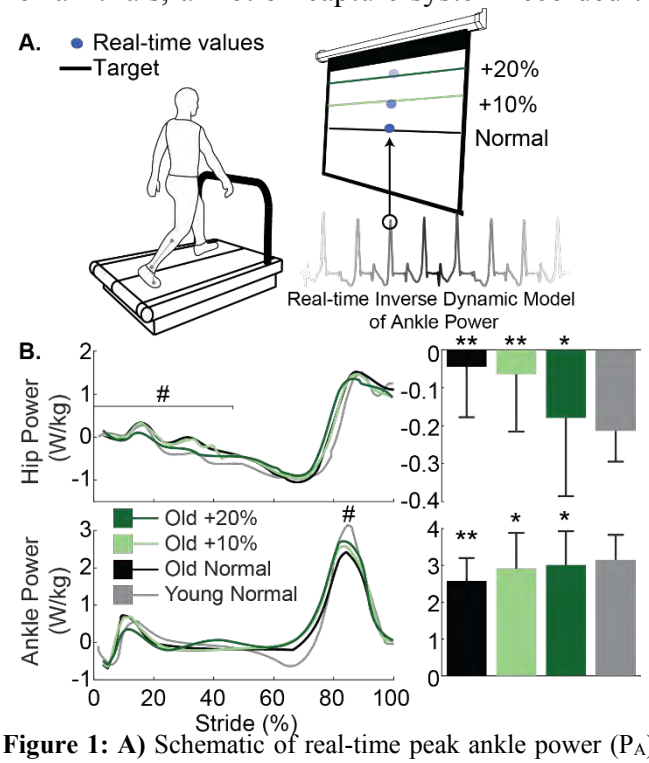


**Figure 1: A)** Schematic of real-time peak ankle power ($P_A$) biofeedback. **B)** Group-mean hip and ankle power plotted against an averaged gait cycle. Pound signs (#) denote a significant main effect of $P_A$ biofeedback ($p<0.05$). Each graph is accompanied by bar graphs indicating group mean (±SD) peaks. Asterisks (*) and double asterisks (**) denote a significant pairwise difference from old and young adults walking normally, respectively.

trajectories of markers placed on subjects' pelvis and lower extremities for estimating joint kinetics. Data reported represents the 20 consecutive strides for which participants were most successful matching prescribed targets. Finally, we again assessed subjects' PWS and FWS to investigate recall. We additionally include normal walking data from 9 healthy young adults (age: 25.1±5.6 years, 4 males/5 females, PWS: 1.30±0.12 m/s) to serve as a reference for comparison.

## RESULTS AND DISCUSSION

Our older adults walked with 21% lower $P_A$ and 79% greater hip power during early to mid-stance compared to their younger counterparts ($p<0.034$). Older adults increased $P_A$ by 13% and 17% when targeting increases of 10% and 20%, respectively (main effect, $p=0.006$), thereby attenuating their $P_A$ deficit compared to young adults (Fig. 1B). Conceptually, older adults could increase $P_A$ through changes in net moment or angular velocity at the ankle. Our older adult subjects increased $P_A$ through modest (+3%) but significant changes to peak ankle moment ($p=0.008$) and nonsignificant changes to angular velocity (+7%, $p=0.157$) (Fig. 2). We also observed larger net ankle moments developed during early to midstance, which may have indirectly contributed to larger than preferred $P_A$ through greater elastic energy storage and return. Greater $P_A$ was also accompanied by up to a 300% reduction in the demand for positive hip power generation during early to mid-stance ($p=0.015$). $P_A$ biofeedback also increased positive ankle joint work ($p=0.001$), total positive leg joint work ($p=0.002$), and $F_P$ ($p<0.001$) (Fig. 2). This latter finding reveals an interesting disconnect in our understanding of push-off in walking: older adults increase $F_P$ without related improvements in $P_A$ [4], but increase $P_A$ with related improvements in $F_P$. Finally, subjects walked overground with 11% faster PWS ($p=0.010$) but no change in FWS when recalling $P_A$ biofeedback.

## CONCLUSIONS

Our results reveal that older adults are capable of increasing $P_A$ through the use of targeted ankle power biofeedback – effects that are accompanied by potentially favorable shifts in hip power generation during early to mid-stance. Moreover, the associated

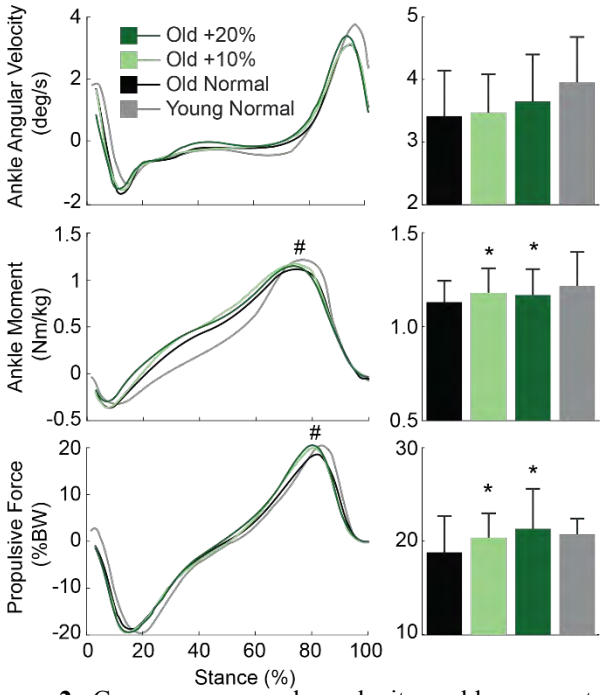


**Figure 2:** Group mean angular velocity, ankle moment, and propulsive force ($F_P$) against an average gait cycle. Asterisks (*) denote a significant main effect of biofeedback ($p<0.05$). Each graph is accompanied by bar graphs indicating group mean (±SD) peaks. Asterisks (*) denote a significant pairwise difference from old adults walking normally.

increase in PWS suggests a functional benefit to increased ankle power output during habitual speed walking. Further work will investigate whether ankle angular velocity alone may be sufficient feedback to modulate $P_A$, an approach more immediately translatable to novel rehabilitation approaches via wearable sensor technologies. Ultimately, targeted biofeedback may complement resistance training to reverse age-associated mobility decline.

## REFERENCES


1. Franz, JR. *Exercise and sport science reviews,* 44(4):129-35, 2016.
2. DeVita, P & Hortobagyi, T. *J Appl Physiol*, 88(5):1804-11, 2000.
3. Ortega, JD & Farley, CT. *J Appl Physiol*. 102(6):2266-73, 2007.
4. Browne, MG & Franz, JR. *Plos One*. In Review, 2018.


## ACKNOWLEDGEMENTS


This work was supported by grants from NIH (R01AG051748) and the UNC University Research Council.

# TRICEPS SURAE MUSCLE-SUBTENDON INTERACTION DIFFERS BETWEEN YOUNG AND OLDER ADULTS

William H. Clark and Jason R. Franz

University of North Carolina and North Carolina State University, Chapel Hill, NC, USA
email: jrfranz@email.unc.edu, web: http://abl.bme.unc.edu

## INTRODUCTION

Mechanical power generated via triceps surae muscle-tendon interaction during walking is largely responsible for the total power needed for forward propulsion and swing initiation [1]. This interaction is made complex by the biological architecture of the Achilles tendon (AT), which consists of distinct bundles of tendon fascicles, known as "subtendons", arising from the gastrocnemius (GAS) and soleus (SOL) muscles [2]. Comparative data and our own *in vivo* evidence alludes to a reduced capacity for sliding between adjacent subtendons compromising the AT in old age. This is functionally important, as subtendon sliding could facilitate independent actuation between individual triceps surae muscles, perhaps augmenting contributions to trunk support and forward propulsion. Indeed, our lab recently found that an age-associated reduction in the capacity for sliding between GAS and SOL subtendons correlated with smaller peak ankle moments and positive work performed during push-off, alluding to unfavorable functional consequences [3]. However, it remains unclear whether age-associated changes at the subtendon level unfavorably affect triceps surae muscle contractile dynamics. Recently, we introduced a novel dual-probe ultrasound imaging approach to reveal that length change differences between the GAS and SOL of young adults during force generation positively correlated with non-uniform tissue displacement patterns in the AT.

Therefore, the purpose of this study was to investigate aging effects on triceps surae muscle-subtendon interaction dynamics using dual-probe ultrasound imaging during a series of ramped isometric contractions. We hypothesized that, compared to young adults, older adults will have (*i*) more uniform Achilles subtendon tissue displacements that (*ii*) are accompanied by more uniform GAS and SOL muscle length change dynamics.

## METHODS

We report data for 9 younger adults (age: 25.1 ± 5.6 years, weight: 69.8 ± 6.9 kg, height: 1.7 ± 0.1 m, 4 females) and, thus far, 6 older adults (age: 74.3 ± 3.4 years, weight: 67.2 ± 9.0 kg, height: 1.7 ± 0.1 m, 4 females). Subjects completed 3 ramped isometric voluntary contractions at each of 5 different ankle angles (spanning 30° plantarflexion to 10° dorsiflexion) using a Biodex (Biodex System 4 Pro), with the knee flexed to replicate that near the push-off phase of walking (~20º). We synchronized two linear array ultrasound transducers to simultaneously record GAS and SOL fascicle kinematics with tissue displacements in their associated tendinous structures (Fig. 1). A 60 mm Telemed Echo Blaster 128 transducer (LV7.5/60/128Z-2) placed over the medial gastrocnemius and soleus of subjects' right leg recorded cine B-mode images at 61 frames/s. Simultaneously, a 38-mm transducer (L14-5W/38, Ultrasonix Corporation, Richmond, BC) operating at 70 frames/s recorded ultrasound radiofrequency (RF) data from a longitudinal cross-section of the right free AT, distal to the SOL muscle-tendon junction and secured via a custom orthotic. Subjects' right foot was barefoot throughout the experiment to facilitate proper placement of the AT transducer.

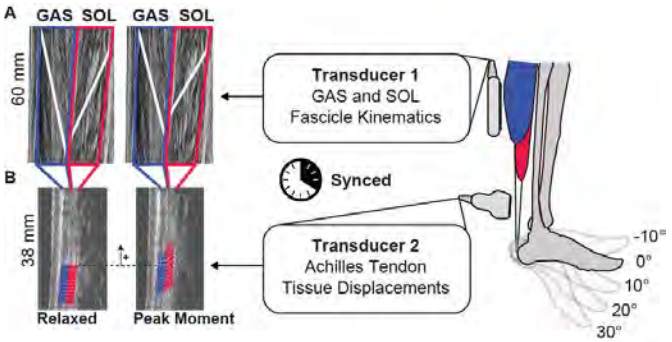


**Figure 1.** Simultaneous ultrasound imaging of the gastrocnemius (GAS), soleus (SOL), and Achilles free tendon. (A) Fascicle lengths and pennation angles derived from cine B-mode images. (B) Custom speckle-tracking of localized Achilles tendon tissue displacements.

Finally, motion capture tracked right ankle and knee joint kinematics and the positions and orientations of both probes.

Available MATLAB routines based on an affine extension to an optic flow algorithm quantified time series of GAS and SOL fascicle lengths and pennation angles (UltraTrack, [4]), which we combined to compute longitudinal muscle lengths. A custom 2D speckle-tracking algorithm estimated localized displacements of AT tendon tissue, which we averaged in two equally sized tendon depths - superficial and deep - corresponding to tendon tissue thought to arise from GAS and SOL, respectively [5]. A repeated measures ANOVA tested for, in part, significant main effects of and interactions between age and ankle angle on GAS-SOL differences in muscle shortening and tendon tissue displacement at peak ankle moment using an alpha level of 0.05.

## RESULTS AND DISCUSSION

For young and older adults, peak isometric plantarflexor moment decreased progressively from dorsiflexion to plantarflexion across the angles tested ($p$<0.01). On average, older adults generated a 21% smaller peak isometric plantarflexor moment than young adults ($p$=0.014). Compared to young adults, average peak muscle shortening was 21% greater for SOL and 81% greater for GAS, while average peak tendon displacement was 18% greater for SOL and 50% greater for GAS in older adults (Fig. 2) – findings fully consistent with functional consequences of increased compliance in older tendon. In addition, consistent with our translational premise, GAS versus SOL differences in muscle contractile behavior and those in subtendon tissue displacements were significant in young but not in older adults. Indeed, as hypothesized, differences between peak GAS subtendon and peak SOL subtendon displacement averaged 44% smaller in older versus young adults (e.g., 77% at 0º, $p$<0.05). Also as hypothesized, differences between peak SOL and peak GAS muscle shortening averaged 58% smaller in older versus young adults (e.g., 65% at 0º, $p$<0.05) (Fig. 2).

## CONCLUSIONS

We reveal that more uniform AT tissue displacements in older versus young adults extend to anatomically consistent and potentially unfavorable changes in muscle contractile behavior – evidenced by smaller differences between GAS and SOL peak shortening during isometric force generation. These findings provide an important biomechanical basis for previously reported correlations between more uniform AT subtendon behavior and reduced ankle moment generation during waking in older adults.

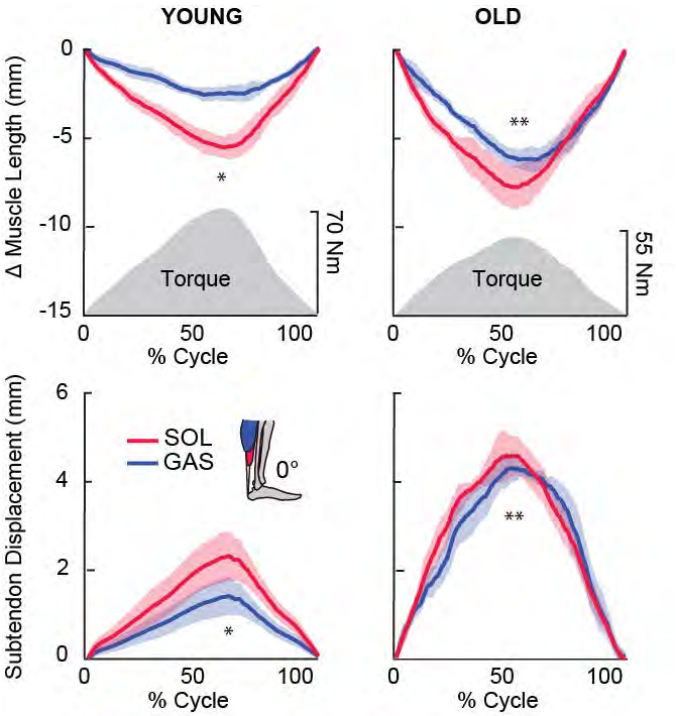


**Figure 2.** Group mean muscle shortening (above) and subtendon displacements (below; proximal positive). Gray shaded regions show the group mean net torque profile during a loading-unloading cycle. Single asterisks (*) indicate significant difference between peak GAS and peak SOL, Double asterisks (**) indicate significant difference between young and old. $p$<0.05 significant.

## REFERENCES


[1] Zelik, K.E., et al. *J Theor Biol*, 2014.75-85.
[2] Szaro, P., et al. *Ann Anat*, 2009. (**6**):586-93.
[3] Franz, J.R., et al. *J Appl Physiol* (1985), 2015. (3):242-9.
[4] Farris, D.J., et al. *Comput Methods Programs Biomed*, 2016.111-8.
[5] Franz, J.R., et al. *Gait Posture*, 2015. (**1**):192-7.


## ACKNOWLEDGEMENTS


We thank Ashish Khanchandani, Hannah Mckenney, and Michael Browne for their assistance with data collection. This study was supported by a grant from NIH (R01AG051748).

# POST-STROKE WALKING MECHANICS USING A SPEED-ADAPTIVE MYOELECTRIC EXOSKELETON CONTROLLER

[1] Emily M. McCain, [1]Tracy N. Giest, [1]Katherine R. Saul, [2]Taylor J.M. Dick and [3]Gregory S. Sawicki

[1] North Carolina State University, Raleigh, NC, USA
[2] University of Queensland, St Lucia, QLD, Australia
[3] Georgia Institute of Technology, Atlanta, Georgia, USA
email: emmccain@ncsu.edu

## INTRODUCTION

Reduced ankle function in post-stroke individuals limits the propulsive 'push-off' power of the paretic limb, resulting in asymmetric gait, reduced walking speed and higher metabolic cost [1]. Powered exoskeletons (exos) offer a promising opportunity to restore mechanical deficits by applying torque at the paretic ankle during the propulsive phase of gait. Previously, a proportional myoelectric ankle exo was shown to increase the paretic plantarflexion moment for stroke survivors walking at 75% of their comfortable overground speed [2]. Despite these improvements, the exos did not reduce the metabolic cost of walking. Researchers suggested exo performance could be limited because the walking speed was restricted to a pace at which exo assistance was not needed. In order to assess the impact of exo assistance on walking speed in stroke populations, we developed a novel, speed-adaptive exo controller [3]. This research extends previous work by: (i) exploring the efficacy of a myoelectric exo controller that automatically modulates the magnitude of propulsive assistance with changes in walking speed for post-stroke populations and (ii) assessing the ability of the controller to improve net average mechanical power output at the paretic ankle, knee and hip joints.

## METHODS

We implemented a speed-adaptive controller designed to mitigate specific limitations of prior myoelectric controllers by including two independent adaptive gains: (1) a gain to map user's soleus muscle activity to peak exo torque (Koller) and (2) a gain to map peak exo torque capacity to walking speed (Giest) [3,4]. The speed-dependent gain ensures the exo outputs ~25% of the maximum normal biological ankle plantarflexion moment at the instantaneous treadmill velocity. The desired exo torque profile was applied by a benchtop motor (Baldor Electric Co) to the carbon-fiber ankle exo through a Bowden-cable transmission system.

Experimental data were collected from six stroke survivors (3 male, 3 female) walking on an instrumented split belt treadmill with and without an exo on their paretic limb. Subjects started by walking at 60% of their preferred speed (n00). At each consecutive minute, the treadmill speed was increased by 0.1 m/s (n01, n02, etc) until the subject's heart rate reached 60% of their heart rate reserve. Kinematic and kinetic data were processed in Visual3D (CMotion, USA) and MATLAB (Mathworks, USA) to determine joint angles and angular velocities. Inverse dynamics was used to calculate joint moments and powers at the ankle, knee, and hip. Average joint powers were calculated at the ankle, knee and hip for five strides [5]. Indirect calorimetry was used to determine metabolic cost during walking (OxyCon Mobile, Carefusion, USA). Statistical significance of peak average ankle power, and net average ankle, knee and hip powers were determined using paired t-tests ($\alpha$=0.05).

## RESULTS AND DISCUSSION

The speed-adaptive controller successfully amplified exo assistance as walking speed was increased, verifying efficacy of the speed-adaptive gain (Figure 1c). Subject averages for maximum paretic ankle power were significantly higher for the exo compared to the no exo condition at all speeds (Figure 1a and 1b) (paired t-test; p=0.04). Since subjects walked until reaching a specific heartrate, statistical power was reduced at high speeds for which the sample size was small (n<4 for n05-n07).

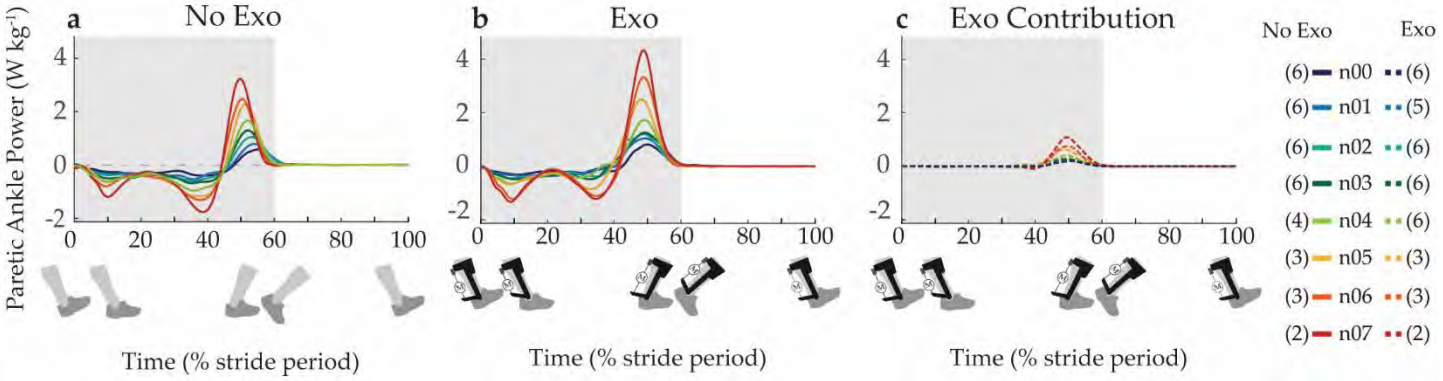


**Figure 1.a** Paretic ankle power in the no exo condition and **1.b** the exo condition with the **1.c** exo contribution isolated. The number of subjects is indicated in parenthesis. The shaded area represents the stance phase of gait.

Net average paretic ankle power was increased for all speeds while wearing the exo, demonstrating improved delivery of net energy at the ankle (paired t-tests; $p<0.05$ for n00-n04) (Figure 2).

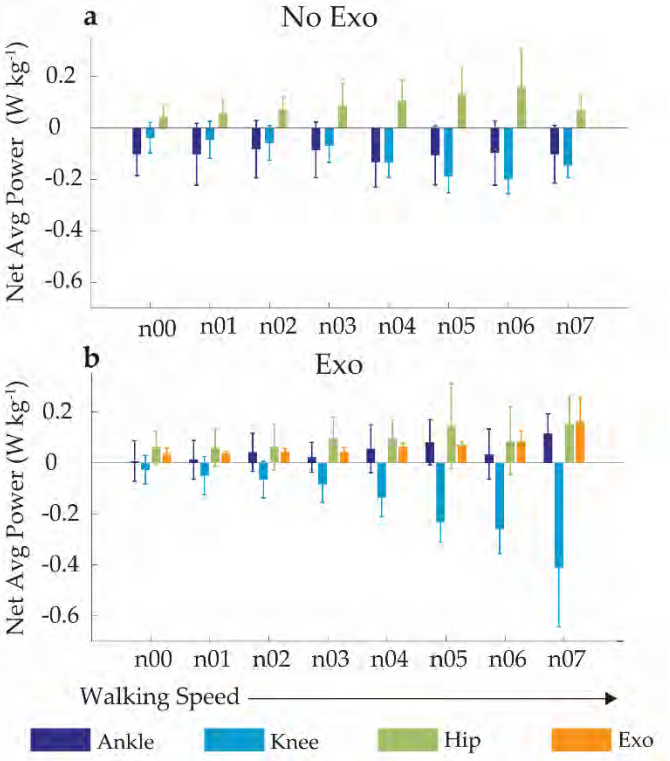


**Figure 2.a** Net average power averaged across subjects for the no exo and **2.b** exo conditions.

Despite these increases in net average ankle power, only two of the subjects experienced a decrease in metabolic cost while wearing the exo compared to the no exo condition, and no statistically significant change was found. One possible explanation is that assistance applied at the ankle may be absorbed by more proximal joints. This explanation is supported by the decrease in net average power seen at the knee in the exo compared to no exo condition (paired t-tests; $p<0.05$ for n00 and n02) (Figure 2).

## CONCLUSIONS

Our speed-adaptive controller successfully increased exo assistance with changes in walking speed for post-stroke individuals. The exo assistance resulted in higher net average power at the paretic ankle. Though we found no significant change in metabolic cost, our exo controller demonstrates the potential of assistive devices to restore paretic limb propulsive power. Future work will examine the interaction between exo assistance, walking speed, distance travelled and gait symmetry between paretic and non-paretic limbs.

## REFERENCES

1. Peterson, CL et al. *J Biomech*. 2010; 43:2348–55.
2. Takahashi, KZ et al. *J NeuroEng Rehab*.2015;12:23
3. Giest, TG et al. *ASB Abstract*, 2016.
4. Koller, JR et al. *J NeuroEng Rehab* 2015; 12:97.
5. Farris, DG et al. *J NeuroEng Rehab* 2015; 12:24.

## ACKNOWLEDGEMENTS

We would like to acknowledge Dr. RW Nuckols for his assistance developing and implementing the controller. Funded by the National Institutes of Health, National Institute for Child Health and Human Development. NIH grant R21 HD072588-01A1 to GSS.

# THE ACHILLES TENDON MOMENT ARM EXHIBITS INDEPENDENT AND COMBINATORY EFFECTS OF JOINT ROTATION AND MUSCLE LOADING

Ashish Khanchandani[1], Hannah McKenney[1], Brianna Arnold[2], William H. Clark[1], and Jason R. Franz[1]

[1]University of North Carolina and North Carolina State University, Chapel Hill, NC, USA
[2]Winston-Salem State University, Winston-Salem NC
email: jrfranz@email.unc.edu web: http://abl.bme.unc.edu

## INTRODUCTION

The Achilles tendon moment arm (ATma), the distance from the tendon's line of action to the ankle joint center, is a critical component of the human musculoskeletal system, transforming triceps surae muscle forces into a moment about the ankle to power functional activities. In contrast to longstanding conventions, we recently discovered that the ATma exhibits highly dynamic variations during walking, which we interpreted to reflect combinatory effects of ankle joint rotation and increases due to triceps surae muscle loading [1] – the latter presumably governed by bulging during force generation. We posit that these variations are functionally meaningful; Lee and Piazza [2] reported that smaller AT moment arms estimated during isolated ankle rotation correlated with slower walking speeds in some older adults. As a biomechanical explanation, we more recently added that age-related reductions in peak ankle moment during push-off were correlated with smaller AT moment arms in older adults [3]. However, due to the complex neuromechanics of muscle-tendon and ankle joint function during walking, our mechanistic understanding of these ATma variations remains fundamentally incomplete.

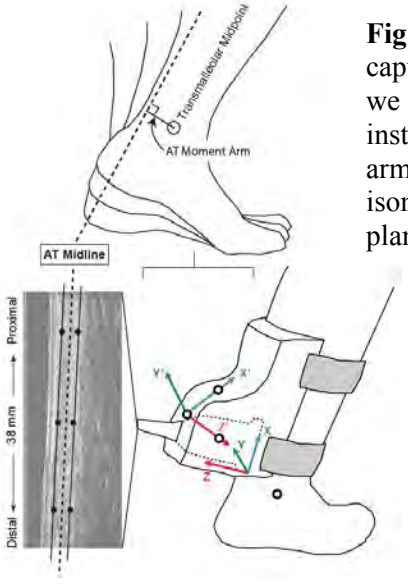


**Figure 1.** Using motion capture guided ultrasound, we estimated the instantaneous AT moment arm during isolated isometric and isotonic plantarflexor contractions.

Therefore, our purpose was to determine the kinematic (*i.e.,* ankle joint rotation) and kinetic (*i.e.,* triceps surae muscle loading) determinants of physiological variations in the Achilles Tendon (AT) moment arm during isolated plantarflexor contractions. We co-registered motion capture estimates of the transmalleolar midpoint with simultaneous cine ultrasound images of the instantaneous AT line of action. We tested the hypothesis that variations in the AT moment arm reflect independent and combinatory effects of ankle joint rotation and triceps surae muscle loading.

## METHODS

11 young adults (age: 25.0 ± 5.4 years, 7F/4M) participated. Subjects were seated in a computer-controlled dynamometer (Biodex Medical Systems, Inc.) with their knee flexed to replicate that near the push-off phase of walking (i.e., ~20°). Subjects performed two series of isolated plantarflexor muscle contractions. In the first (effect of muscle loading while controlling for ankle angle), subjects performed three ramped isometric voluntary contractions at five ankle joint angles spanning 10º dorsiflexion to 30º plantarflexion, each separated by at least one minute and presented in random order. In the second (effect of ankle angle while controlling for muscle loading), subjects performed three isotonic concentric contractions over their range of motion at each of three ankle joint moments (i.e., 25%, 50%, and 75% of their peak 0° isometric ankle joint moment). During all trials, a custom orthotic positioned a 38 mm linear array transducer (L14-5W/38, Ultrasonix Corporation) over subjects' right Achilles free tendon, on average ~6 cm superior to the calcaneal insertion. We recorded ultrasound radiofrequency (RF) data from a longitudinal cross-

section of the AT. We manually tracked the AT midline from B-mode images created from the RF data using previously published procedures [2]. Finally, we calculated instantaneous variations in subjects' ATma as the perpendicular distance between the AT midline and the transmalleolar midpoint, estimated using marker data collected using eight cameras from a 14-camera motion capture system (Motion Analysis, Corp.).

## RESULTS AND DISCUSSION

As hypothesized, and consistent with measurements made during walking, we found here that the Achilles tendon moment arm (ATma) exhibits independent and combinatory effects of ankle joint rotation and triceps surae muscle loading. In the absence of muscle loading during the isometric tasks, we found that the ATma became systematically smaller with increasing ankle plantarflexion ($p<0.001$, Fig. 2A). For example, at rest, the ATma was 7% smaller on average at 30° plantarflexion than at 10° dorsiflexion. In contrast, at maximum isometric activation, we found no significant effect of ankle joint angle on the ATma ($p=0.496$, Fig. 2B). We similarly found no significant main effect of ankle joint rotation across the range of motion tested during isotonic contractions performed at ≥25% maximum isometric torque ($p=0.218$, Fig. 2D). We interpret these findings to suggest that while ankle joint rotation systematically influences the ATma, a result fully consistent with prior reports, muscle loading substantially attenuates those effects. One possible explanation is that the effects of ankle joint rotation on the ATma, at least those with increasing plantarflexion, are governed primarily by tendon slack and tendon curvature – factors that are themselves both attenuated by triceps surae muscle loading. Indeed, we acknowledge that our range of dorsiflexion angles was limited.

Triceps surae muscle loading also independently increased the ATma. During ramped isometric contractions, the ATma increased by as much as 8% compared to resting values (Fig. 2C). However, this effect reached significance only for the two most plantarflexed ankle positions (i.e., 20° and 30°). We also found a significant main effect of muscle loading on the ATma during concentric isotonic contractions (Fig. 2D). Post-hoc comparisons revealed this was driven by modest but progressive increases in ATma from 25% maximum isometric torque to 50% ($p=0.032$) and again to 75% ($p=0.017$) – effects that held across the range of motion tested.

## CONCLUSIONS

Our findings reveal that the Achilles tendon moment arm (ATma) exhibits complex independent and combinatory effects of ankle joint rotation and triceps surae muscle loading – results with clear implications for the study of elderly gait and the musculoskeletal modeling community. This outcome is also fully consistent with our earlier interpretations of the mechanisms governing physiological variations in the ATma observed during walking.

## REFERENCES


1. Rasske et al., *CMBBE* **20(2)**: 201-5, 2017.
2. Lee and Piazza, *J Biomech* **45**, 1601-1606, 2012.
3. Rasske and Franz, *J Biomech* (in revision)


## ACKNOWLEDGEMENTS


Funded by NIH (R01AG051748) and the National Center for Simulation in Rehabilitation Research.


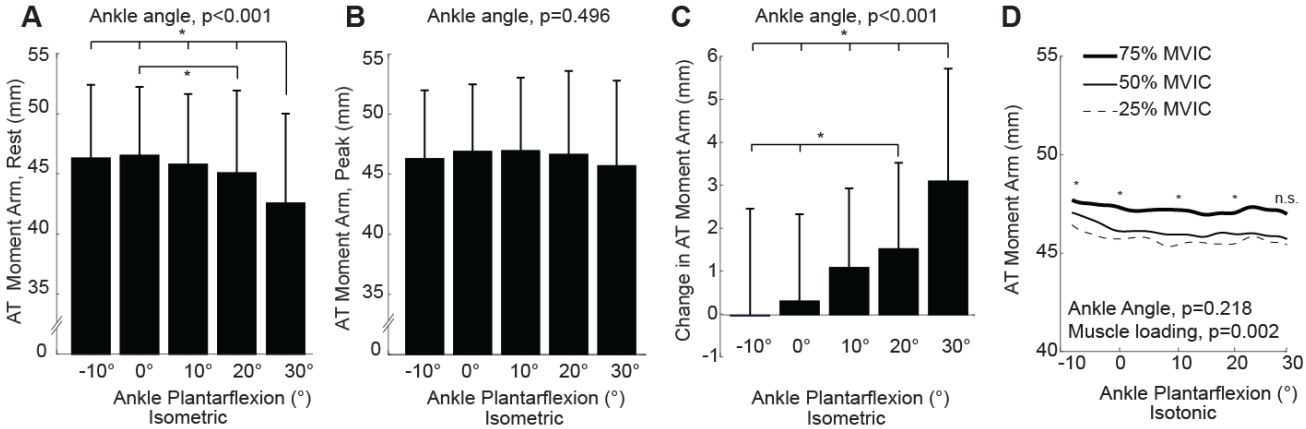


**Figure 2.** Group average (standard deviation) effects of ankle joint rotation and triceps surae muscle loading during maximum isometric (A-C) and concentric isotonic (D) contractions performed in isolation using a dynamometer.

# ACTIVATION-DEPENDENT CHANGES IN SOLEUS LENGTH-TENSION BEHAVIOR AUGMENT ANKLE JOINT QUASI-STIFFNESS

William H. Clark and Jason R. Franz

University of North Carolina and North Carolina State University, Chapel Hill, NC, USA
email: jrfranz@email.unc.edu, web: http://abl.bme.unc.edu

## INTRODUCTION

The triceps surae (i.e., gastrocnemius and soleus) muscle-tendon units are functionally important in governing walking performance, acting to regulate mechanical behavior of the ankle joint through the interaction between active muscle and passive elastic structures [1]. Ankle joint quasi-stiffness, defined as the slope of the relation between ankle moment and ankle rotation, is a useful aggregate measure of this presumably complex mechanical behavior [2]. For example, quasi-passive lower limb prostheses with impedance control methods have garnered attention and their designs are benchmarked against the quasi-stiffness of the biological ankle joint [3]. In walking, ankle joint quasi-stiffness systematically changes with walking speed and positively correlates with positive work performed about the ankle during push-off [3]. Those findings reflect a fundamental assumption that the control of triceps surae muscle behavior can functionally augment ankle joint quasi-stiffness via changes in activation. However, while entirely intuitive, this assumption lacks direct empirical evidence that, in addition to its biological relevance, could be vital in designing appropriate control systems for powered prostheses [2].

The purpose of this study was to couple dynamic ultrasound imaging with electromyographic biofeedback to quantify activation-dependent modulation of soleus muscle length-tension behavior and its role in augmenting ankle joint quasi-stiffness. We first hypothesized that soleus muscle stiffness and ankle joint quasi-stiffness would increase with increasing muscle activation. We also tested the null hypothesis that activation-dependent changes in soleus muscle stiffness would be proportional to and correlate with those in ankle joint quasi-stiffness.

## METHODS

We report data for 10 subjects (age: 24.5 ± 5.4 yrs, mass: 74.7 ± 12.7 kg, height: 1.8 ± 0.1 m, 4 females). Subjects first completed 3 isometric voluntary plantarflexor contractions (IVCs) at a neutral ankle (i.e., 0º) in a dynamometer (Biodex Medical Systems, Inc.), from which we extracted a reference maximum voluntary activation from a wireless electrode (Delsys, Inc.) placed over the soleus muscle. Subjects then completed 3 eccentric isokinetic plantarflexor contractions between 20º plantarflexion and 15º dorsiflexion at 30º/sec both passively and at each of 2 prescribed activation levels (25% and 75% reference maximum activation), all presented in fully randomized order. To match prescribed activations, subjects watched a screen on which we projected real-time visual electromyographic (EMG) biofeedback showing their instantaneous soleus activation (250 ms moving average) with target values based on the reference maximum activation determined earlier (Fig. 1). Subjects received at least one minute of rest between trials. A 60 mm Telemed Echo Blaster 128 transducer (LV7.5/60/128Z-2) placed over the mid-belly of subjects' right soleus recorded cine B-mode images of a longitudinal cross-section at 61 frames/s. Simultaneously, motion capture-guided ultrasound from a second transducer (L14-5W/38, Ultrasonix Corporation) placed over the Achilles free tendon estimated the moment arm of the line of action of

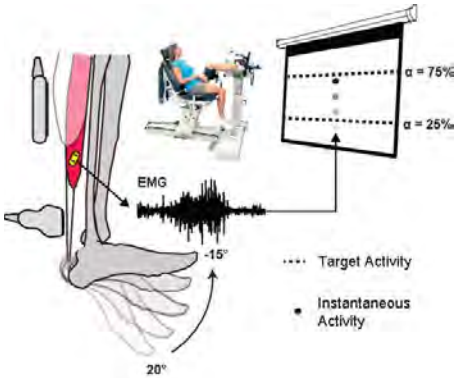


**Figure 1.** We used visual biofeedback to prescribed muscle activations (α) during eccentric isokinetic plantarflexor contractions while cine ultrasound imaging captured soleus muscle length changes.

soleus muscle force for each subject using previously published techniques [4]. Available MATLAB routines quantified time series of soleus fascicle length and pennation angle [5], which we combined to compute length change along the line of action of the soleus. To calculate "muscle stiffness", we resolved net triceps surae muscle force by dividing subjects' net ankle moment by their measured moment arm [4]. We then estimated soleus muscle force by scaling triceps surae force by the relative physiological cross-sectional area attributed to the soleus (i.e., 63%) [6]. For each subject, we defined: (*i*) muscle stiffness as the change in soleus muscle force divided by the change in muscle length, and (*ii*) ankle joint quasi-stiffness as the change in ankle moment divided by the change in ankle angle.

## RESULTS AND DISCUSSION

In the absence of muscle activity, we found relatively negligible values of soleus muscle stiffness ($k_M$) and ankle joint quasi-stiffness ($k_A$) across the range of ankle rotation observed during walking. In contrast, $k_M$ and $k_A$ increased significantly with increased muscle activation ($p<0.05$). On average, $k_M$ was 15 N/mm during passive rotation, 118 N/mm during the 25% IVC condition, and 204 N/mm during the 75% IVC condition (Fig. 2A). On average, $k_A$ was 24 Nm/rad during passive rotation, 154 Nm/rad during the 25% IVC condition, and 213 Nm/rad during the 75% IVC condition (Fig. 2B). However, these activation-dependent changes were made complex by the interaction between active muscle and passive elastic structures. Conceptually, from 0% to 25% IVC, increased muscle activity should augment $k_A$ directly by increasing $k_M$ and indirectly by engaging series elastic tendon (i.e., $\Delta k_A > \Delta k_M$). Consistent with this premise, although highly correlated ($R^2=0.87$), we found that the sensitivity (i.e., slope) of $k_A$ to altered activation averaged 25% greater than that of $k_M$ from 0% to 25% IVC ($p=0.069$, Fig. 2C). Thereafter, the contribution of tendon stiffness to $k_A$ is independent of activation; further increases in muscle activity should augment $k_A$ only by increasing $k_M$. Indeed, compared to changes seen with 25% IVC, $k_A$ was significantly less sensitive to further increasing activation to 75% IVC ($p=0.016$) – a change indistinguishable from that of $k_M$ ($p=0.23$) (Fig. 2C). Surprisingly, $k_M$ was also less sensitive to further increasing activation to 75% IVC ($p=0.025$).

## CONCLUSIONS

We present *in vivo* evidence that ankle joint quasi-stiffness can be directly modulated via activation through changes in soleus muscle length-tension behavior. However, this modulation is more complex than previously appreciated – reflecting combinatory effects of active muscle and passive elastic tissues. Our findings have substantial implications for understanding human locomotor behavior and the design of impedance-based powered prostheses.

## REFERENCES


[1] Zelik, K.E., et al. *J Theor Biol*, 2014.75-85.
[2] Rouse, E.J., et al. *IEEE Trans Biomed Eng*, 2013. 2:562-8.
[3] Shamaei, K., et al. *PLoS One*, 2013. (**3**):e59935.
[4] Rasske, K., et al. *Comput Methods Biomech Biomed Engin*, 2017. (2):201-205.
[5] Farris, D.J., et al. *Comput Methods Programs Biomed*, 2016.111-8.
[6] Morse, C.I., et al. *Acta Physiol Scand*, 2005. (**3**):291-8.


## ACKNOWLEDGEMENTS


Supported by a grant from NIH (R01AG051748).


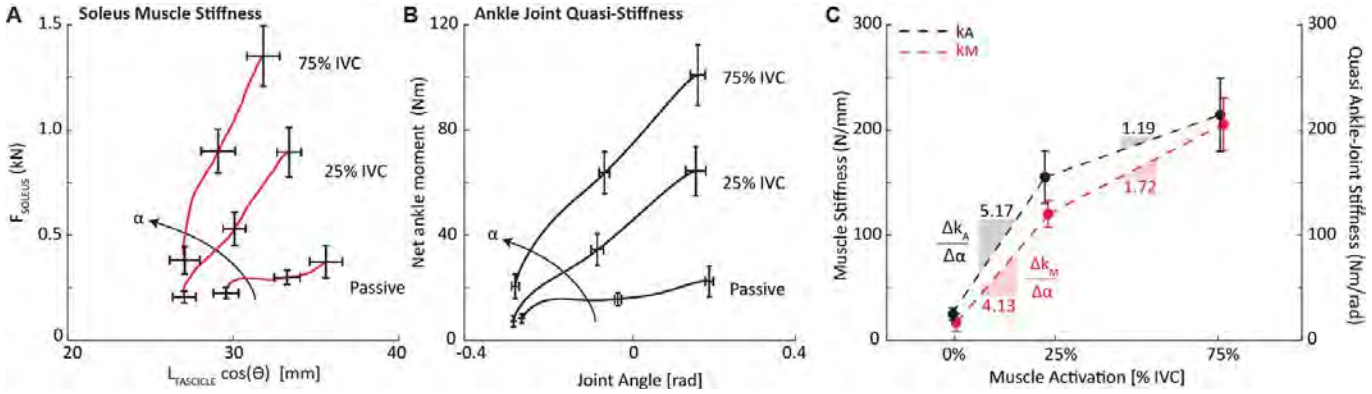


**Figure 2.** Activation-dependent changes in muscle ($k_M$) and quasi-ankle joint ($k_A$) stiffness. (A) Group mean change in soleus muscle force ($F_{Soleus}$) versus longitudinal soleus muscle length ($L_{fascicle}$ cos Θ) as a function of activation (Θ: pennation). (B) Group mean change in net ankle moment versus joint angle as a function of activation. (C) Activation-dependent $k_M$ and $k_A$ from 0% to 25% and 25% to 75% IVC. Bars represent ± standard error.

# OLDER ADULTS OVERCOME THEIR DEFICITS TO YOUNG ADULTS WHEN PROPULSIVE DEMANDS OF WALKING ARE INCREASED TO THEIR MAXIMUM

Katie A. Conway, Randall Bissette, and Jason R. Franz

University of North Carolina at Chapel Hill and North Carolina State University, Chapel Hill, NC, USA
email: kaconway@unc.edu, web: http://abl.bme.unc.edu

## INTRODUCTION

Reduced push-off intensity during walking, arising from diminished plantarflexor mechanical output and thus propulsive force generation, plays an important role in age-related mobility impairment [1]. Unfortunately, conventional interventions aimed at enhancing ankle power generation (e.g., resistance training) seem to convey benefits only during maximum speed walking [2]. Thus, improving maximum muscular capacity may fail to alter the instinctive utilization of that capacity, with limited improvements for habitual walking. As a potential explanation, evidence suggests that older adults retain the capacity to enhance push-off performance, for example to walk uphill or with biofeedback [3-4]. Thus, our working hypothesis is that many older adults retain a 'propulsive reserve' during normal walking that goes underutilized for reasons that are poorly understood (e.g., **Fig. 1A**). Understanding the emergence of these reserves, and thus the functional utilization of propulsive capacity during walking, is a critical step toward the strategic and discriminate prescription of resistance training complemented by innovative alternative therapies to restore walking ability in our aging population.

Therefore, our purpose was to gain an improved joint-level understanding of the utilization of propulsive capacity in older adults during walking, and thereby the availability of propulsive reserves, with a special emphasis on the plantarflexor muscles. We leveraged a motor-driven impeding force system and maximum speed walking to systematically increase the propulsive demands of walking to their maximum. We hypothesized: (*i*) that older adults would exhibit a diminished push-off intensity compared to their younger counterparts, but (*ii*) that older adults' propulsive reserve would allow them to overcome those deficits when the propulsive demands of walking are increased to their maximum.

## METHODS

Twelve healthy older adults participated (age: 75.0±4.6 years, height: 1.71±0.1 m, body mass: 68.6±11.1 kg, 5M/7F). We first recorded subjects' preferred (1.28±0.2 m/s) and maximum (1.89±0.1 m/s) walking speeds using an instrumented walkway. Subjects then walked on a dual-belt instrumented treadmill (Bertec, Corp.) for 1 min at their preferred speed ("Pref"). In another

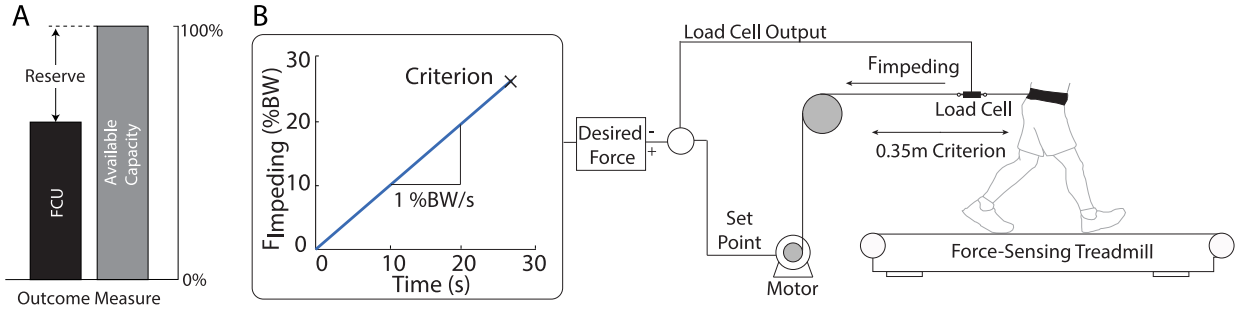


**Figure 1.** (A) Schematic showing our representation of propulsive reserves, shown here as the difference between functional capacity utilized (FCU) and maximum available capacity. (B) A motor-driven, feedback controlled impeding force system including load cell and motor increased the demand for propulsive forces at a rate of 1% BW/s until we observed an inexorable 0.35 m posterior displacement of the subject's pelvis.

trial, subjects walked on the treadmill at their maximum overground walking speed, which they maintained for approximately 10 s ("Fast"). Subjects also wore a waist belt that connected to a feedback-controlled, motor-driven system that prescribed horizontal impeding forces according to instantaneous measurements from a load cell (**Fig. 1B**). Specifically, while subjects walked at their preferred speed on the treadmill, a real-time controller increased the impeding force at a constant rate of 1 %BW/s ("Ramp"). The trial ended following a 0.35 m inexorable posterior translation of the subjects' center of mass, monitored using the motor's encoder. For all treadmill trials, we recorded the 3D trajectories of retroreflective markers on the pelvis and lower limbs using motion capture (Motion Analysis, Corp.) and used inverse dynamics to estimate leg joint moments and powers. Finally, we compared to reference data from young adults (24.5±5.5 years) walking at their preferred speed (1.35±0.2 m/s, p=0.281 vs. old).

## RESULTS AND DISCUSSION

Older adults walked normally with 14% smaller peak propulsive forces (p=0.012) and 19% smaller peak ankle power (p=0.022) than young adults. However, these deficits disappeared as the propulsive demands of walking increased (**Fig. 2**). Compared to normal walking, older adults increased their peak propulsive force by an average of 42% and 68% during maximum speed and maximum ramp, respectively. (p<0.001). Interestingly, this ability to increase propulsive force to its maximum during preferred speed walking is nearly identical to that found previously for older adults walking at a 9° uphill grade (i.e., +69%), suggesting a functionally limiting environmental demand for older adults [3]. Peak ankle power, but not peak moment, also increased during these conditions, by 59% and 22% compared to Pref, respectively (p<0.021) (**Fig. 2**).

## CONCLUSIONS

Using a ramped impeding force protocol, we have discovered preliminary evidence that older adults' propulsive reserve allows them to overcome apparent age-related deficits in push-off intensity, at least for peak propulsive force and ankle power generation. Interestingly, of the outcome measures used to characterize push-off intensity, peak ankle moment increased when walking faster but not when generating maximum propulsive forces. The emergence of propulsive reserves in elderly gait may facilitate the more discriminate prescription of interventions aimed at enhancing walking ability by increasing push-off intensity in older adults.

## REFERENCES


1. Kerrigan et al. *Arch Phys Med Rehab*, **79**, 1998.
2. Beijersbergen et al. *Gait Posture*, **52**, 2017.
3. Franz. *Exer Sport Sci Rev*, **44**, 2016.
4. Franz and Kram. *J Biomech*, **46(3),** 2013.


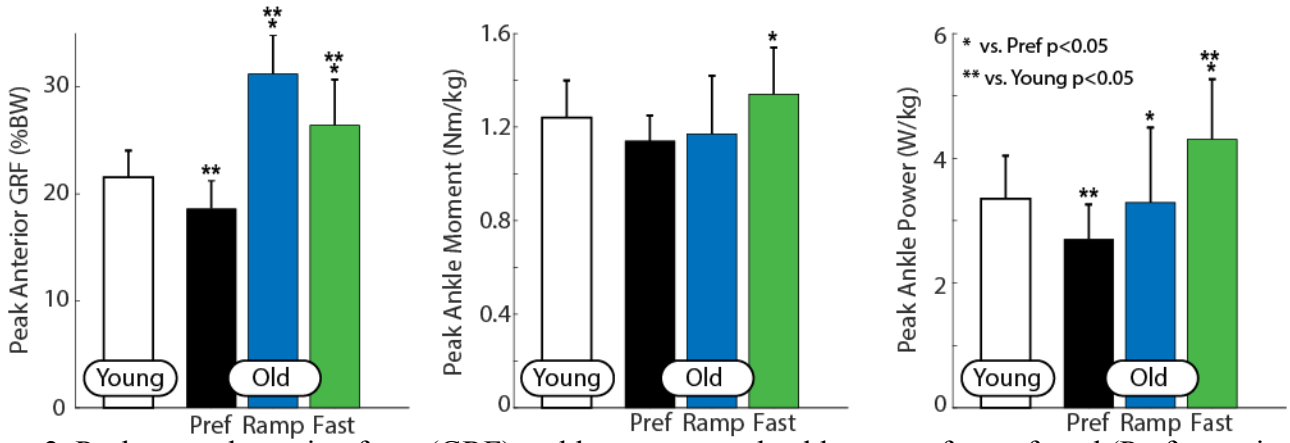


**Figure 2.** Peak ground reaction force (GRF), ankle moment and ankle power for preferred (Pref), maximum ramp (Ramp) and maximum speed (Fast) trials, compared to reference normal walking data for young adults (Young).

# EFFECT OF ENVIRONMENT ON GAIT AND GAZE DURING WALKING IN OLDER ADULT FALLERS

[1] Lisa A. Zukowski, [2] Carol Giuliani, and [2] Prudence Plummer

[1] High Point University, High Point, NC, USA
[2] University of North Carolina at Chapel Hill, Chapel Hill, NC, USA
email: lzukowsk@highpoint.edu

## INTRODUCTION

Environmental hazards have been identified as a major cause of falls in healthy, older adults [1], yet traditional fall-risk assessments do not adequately take into account the role of distractions and hazards experienced in everyday life. Compared to the low-distraction setting of a laboratory, the real world is a highly distracting environment with constant demands on visual attention to avoid hazards and falling. A better understanding of the differences between older adults at risk of falling and older adult non-fallers during walking in the real world, relative to a lab setting, may improve fall-risk evaluation.

The purpose of this project was to identify the effect of the environment on gait and gaze behavior during walking in older adult fallers relative to non-fallers. We hypothesized that 1) relative to the lab, in the real world older adults would exhibit greater gait variability, greater fixation durations (indicative of less or slower active scanning), and more frequent fixations on the travel path, and 2) the environmental influence on gait and gaze would be more pronounced in fallers than non-fallers.

## METHODS

Thirteen older adult fallers (76.8±9.4 years of age, 10 females, 16.8±3.3 years of education) and 13 older adult non-fallers (78.3±7.3 years of age, 9 females, 16.7±2.3 years of education) were recruited from the local community. Fallers were defined as those reporting 2 or more falls within the past 12 months; non-fallers reported no falls in the last 12 months.

Participants performed 2 walking task trials for 1 minute in both a real-world environment (busy hospital lobby) and laboratory setting. We recorded spatiotemporal gait parameters using the LEGSys 5-node wireless ambulatory system (100 Hz, Biosensics, Cambridge, MA) and gaze behavior using wireless eye tracking glasses (60 Hz, SensoMotoric Instruments, Boston, MA) during each walking task. The surrounding environment was recorded with a video camera during each walk.

The dependent variables were coefficient of variation of stride length and stride duration, stride velocity, percentage of total time fixating on 6 areas of interest (AOIs, i.e., far environment (FE), far walking path (FW), far people (FP), near environment (NE), near walking path (NW), and near people (NP)), and average duration of fixation on the 6 AOIs. For each dependent variable, we computed the average across the 2 walking trials in each environment. From each video recording, we quantified the environmental busyness during each walk (number of people in and outside of participant's walking path).

Independent samples t-tests were utilized to compare fallers and non-fallers based on age, sex, and years of education. A paired samples t-test was utilized to compare the environmental busyness of the lab relative to the lobby, and independent samples t-tests were utilized to compare the environmental busyness between fallers and non-fallers in both testing environments. A repeated measures ANOVA was utilized to compare average walking performance and gaze behavior for fallers and non-fallers in the laboratory and hospital lobby settings (Group x Environment). All statistical procedures were performed using SPSS 24 and $\alpha$=0.05.

## RESULTS AND DISCUSSION

There were no significant differences between fallers and non-fallers in terms of age, sex, or years of education. Thus, the only difference between the two groups was fall history.

The real-world environment was significantly busier (22.4±7.7 individuals) than the lab setting (1.1±1.0 individuals) in terms of people walking in and outside of the walking path ($p<0.001$). However, there were no significant differences in busyness of either environment between fallers and non-fallers. Thus fallers and non-fallers were presented with similarly challenging lab and real-world environments to navigate.

In contrast to our hypothesis, we did not find a significant effect of environment on gait variability or gait speed. In other words, there were no differences in gait between the environments. However, non-fallers walked 0.2 m/s faster than fallers ($p=0.03$), which is in agreement with previous research that shows that a fall history is related to slower walking speeds [2]. There were no differences between the groups in terms of gait variability.

We found a significant effect of environment on gaze behavior, but in contrast to our hypothesis, older adults fixated 32.3% less frequently ($p<0.001$) and for 67.0 ms less time ($p=0.001$) on FW and 6.6% less often on the NW ($p=0.002$) in the lobby relative to the lab (Fig. 1). From the lab to the lobby, they also fixated 38.8% more frequently on FP and 2.27% more often and for 139.1 ms longer on NP (all $p<0.001$, Fig. 1). Thus participants appeared to prioritize visually attending to people within and adjacent to their walking path, who represent environmental hazards, as opposed to their actual walking path or more varied visual scanning of the environment. This finding is supported by the work of Di Fabio et al. [3] who determined that age-related changes in spatial information processing impact fixation duration on hazards within the walking path. Our secondary hypothesis was partially corroborated by the greater 214.8 ms decrease in time spent fixating on the NE in the lobby by fallers, relative to the 38.8 ms decrease by non-fallers ($p=0.01$, Fig. 1). Fallers may have been less comfortable in diverting attention from urgent environmental hazards to look at the near environment in the lobby than non-fallers.

## CONCLUSIONS

Gait performance did not differ between the environments. However, relative to the lab, in a real-world setting older adults fixated more frequently and for longer on people in their environment, and fallers decreased their fixation time on their near environment. Thus, the addition of moving hazards and distractions to fall-risk assessments may provide new means of evaluating fall-risk status.

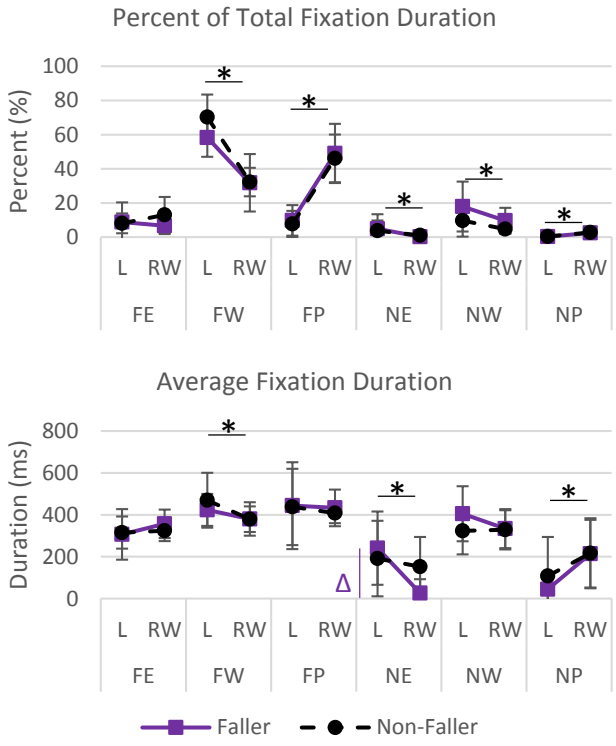


**Figure 1**: Gaze behavior on the 6 AOIs (FE, FW, FP, NE, NW, and NP) of fallers and non-fallers in the lab (L) and real-world (RW) environments. Significant differences between environments (*) and a Group x Environment interaction effect (Δ) are indicated.

## REFERENCES


1. Rubenstein and Josephson. *Clin Geriatr Med*. **18**, 141-58, 2002.
2. Verghese et al. *J Am Geriatr Soc*. **50**, 1572-6, 2015.
3. Di Fabio et al. *Neurosci Lett*. **339(3)**, 179-82, 2003.


## ACKNOWLEDGEMENTS


The project described was supported by the National Center for Advancing Translational Sciences (NCATS), National Institutes of Health, through Grant Award Number UL1TR001111. The content is solely the responsibility of the authors and does not necessarily represent the official views of the NIH.